Method for Calculating the PCS Film Coverage Input for the AP600 Containment DBA Evaluation Model

May 15, 1996

R. P. Ofstun
D. R. Spencer
J. Woodcock
S. K. Slabaugh
M. Sredzienski

Executive Summary

The purpose of this chapter of the Applications Report is to describe the method used to calculate the film coverage input for the AP600 containment DBA evaluation model. A mechanistic model for predicting film stability is described. A bounding multiplier value for the film stability model is based on data from the PCS tests. The estimated AP600 range of film coverage parameters is covered by the PCS test data for film on the prototypical surface. The film stability model is used to conservatively calculate the PCS film runoff flow rate as a function of time. The difference between the gravity driven PCS flow rate and the predicted runoff flow rate is input to the evaluation model. The delay in application of the film flow rate and the film coverage area and wetted perimeter input values are based on data from the full scale Water Distribution Tests. The results of sensitivity analyses with the evaluation model are presented. The calculated peak pressure decreases as the film flow rate increases, but is not sensitive to changes in the coverage area or location. The method used to calculate the film coverage input for the AP600 containment DBA evaluation model is shown to be conservative.

Table of Contents

8.1 Introduction

The energy released to the containment atmosphere following a postulated accident in the AP600 is removed from the exterior shell surface by a combination of convection, radiation and evaporation. Evaporation provides the primary (approximately 80%) source of energy removal.

The water required for evaporation begins flowing under the influence of gravity from a tank located on top of the containment structure shortly after a PCS actuation signal occurs. The water fills a central distribution bucket, spills onto the dome and begins to spread and heat up on the nearly horizontal surface at the top of the dome. The water coverage at the top of the dome is influenced primarily by surface irregularities caused by plate misalignment during welding.

To produce a more even coverage of the dome and vertical sidewalls of the shell, the water is redistributed by a series of weirs (one located at the [ ]^{a,c} radius and another at the [ ]^{a,c} radius on the dome). A detailed description of the weirs is given in Ref. 2. The streams of water flowing over the weirs form multiple wet "stripes" of film. The width (wetted perimeter) of the film stripes increases due to the area divergence on the dome. The combination of area divergence and evaporation causes the film thickness to decrease as the stripes flow down the surface of the dome and onto the vertical sidewall of the containment shell. The wetted perimeter of the evaporating film is dependent on the stability of the film. The film stability decreases as the film thickness decreases and as the temperature difference across the film increases. When the film becomes unstable, a dry spot forms, and the wetted perimeter decreases.

The shell evaporation rate is a function of the shell heat flux, wetted perimeter and film flow rate, all of which are interdependent and vary with time and position. The internal heat flux to the shell is dependent on the mass and energy release rate and the condensation rate. The shell heat flux decreases with time and increases with increasing elevation. The gravity driven water flow rate is dependent on the standpipe design and the head of water in the storage tank, and also decreases with time. The film flow rate and wetted perimeter decrease with time and change with elevation as spreading and evaporation occur.

The containment DBA evaluation model requires an input water flow rate along with elevation dependent water coverage area and wetted perimeter input values to compute the evaporation rate from the shell. Because the evaluation model uses constant values for the water coverage area and wetted perimeter input at each elevation, the water flow rate input must account for changes in the evaporation rate with time.

The purpose of this report is to describe the methodology utilized to define a conservative water flow rate input for the AP600 containment DBA evaluation model. The approach is outlined below:

1. Examine PCS test data with respect to film coverage to determine: how the film stripes form, how the coverage is affected by the actual geometry (weirs, maximum allowable

surface irregularities), and how the coverage varies over the range of post accident AP600 containment operating conditions (heat flux, temperature, film flow rate).

2. Select a model for predicting the film coverage and compare it with test data to show how it can be conservatively applied to calculate the maximum runoff flow rate from the containment shell.

3. Subtract the conservatively calculated runoff flow rate from the gravity driven water flow rate for input to the AP600 containment evaluation model.

8.2 PCS Test Data Evaluation

The AP600 containment shell surface will be coated with an inorganic zinc compound for corrosion protection. Measurements and/or observations of film coverage on the prototypical surface were made in several PCS tests. This section provides a description of each test and a summary of results.

The important parameters for characterizing water coverage are the inlet and exit film flow rate, the inlet and exit film temperature, and the inlet, exit and average heat flux. Table 8-1 presents a summary of the ranges of the various dimensional and non-dimensional test parameters for all of the PCS wetting tests.

8.2.1 Water Film Formation Tests

The Water Film Formation Tests (Ref. 8.1) were performed to show the wettability of the selected inorganic zinc coating for the AP600 containment shell and to characterize general requirements for forming a water film over a large surface area. An unheated, 8-ft. long, 4-ft. wide steel plate, which had been painted with the selected inorganic zinc coating, was placed on a pivoting frame to simulate the various angles on the containment dome and sidewall. A stream of water was applied to the center top edge of the plate to see how it would spread to cover the surface.

With a flow rate of 1 gpm from a 1/2-inch diameter tube pointed perpendicular to the surface, the water spread to form a 1-ft. wide stripe of film down the 8-ft. length. These same results were obtained at plate angles of 90° and 11° from horizontal. The film thickness was not uniform near the point of application; it was thinnest just below the application point and thicker on both sides. The film stripe continued to spread (more slowly as the surface became more vertical) and a very thin, wet region was created at the edges as the film traveled downward.

Various film spreading mechanisms were also investigated. A dam and weir system was found to be the most effective in distributing the water to create a wavy laminar film over the entire width of the plate.

Table 8-1 - Ranges of the Film Coverage Parameters in the PCS Tests

a,c

8.2.2 Water Distribution Tests

The Water Distribution Tests were used to determine the water coverage as a function of the flow rate on the prototypical surface and to determine the time to establish steady state coverage on the AP600. A full scale test section, representing a 1/8 sector of the containment dome and a portion of the vertical sidewall, was built. The test section included both meridional and circumferential joints with the maximum allowable plate misalignment. There was no source of heat to simulate energy removal by evaporation for these tests. Various weir distribution systems were tested. The final weir design was tested in phase 3 of the Water Distribution Tests (Ref. 8.2).

The water coverage for a flow rate of 27.5 gpm (equivalent to 220 gpm on the AP600) was estimated to be [ ]^{a,c} from the top of the dome down to the first weir, based on a review of the video tapes for the phase 3 water distribution tests (with the improved weir design). About [ ]^{a,c} of the vessel was wet between the first and second weirs and the entire vessel was wet at the bottom of the test section. The coverage was measured at the springline ([ ]^{a,c} radius at the top of the vertical sidewall) and just above the second weir (at the [ ]^{a,c} radius). Only the widths of the visibly flowing water stripes were measured. The phase 3 test data is summarized in Table 8-2.

Table 8-2 - Summary of the Water Distribution Tests

a;c

[ ]

Figure 8-1 presents the measured coverage at the springline and just above the second weir as a function of the applied water flow rate for all of the Phase 3 Water Distribution Tests. The coverage decreases as the applied flow rate decreases. The flow rate was not adjusted to account for the water lost at sampling points upstream of the springline. This correction would shift the data points slightly to the left.

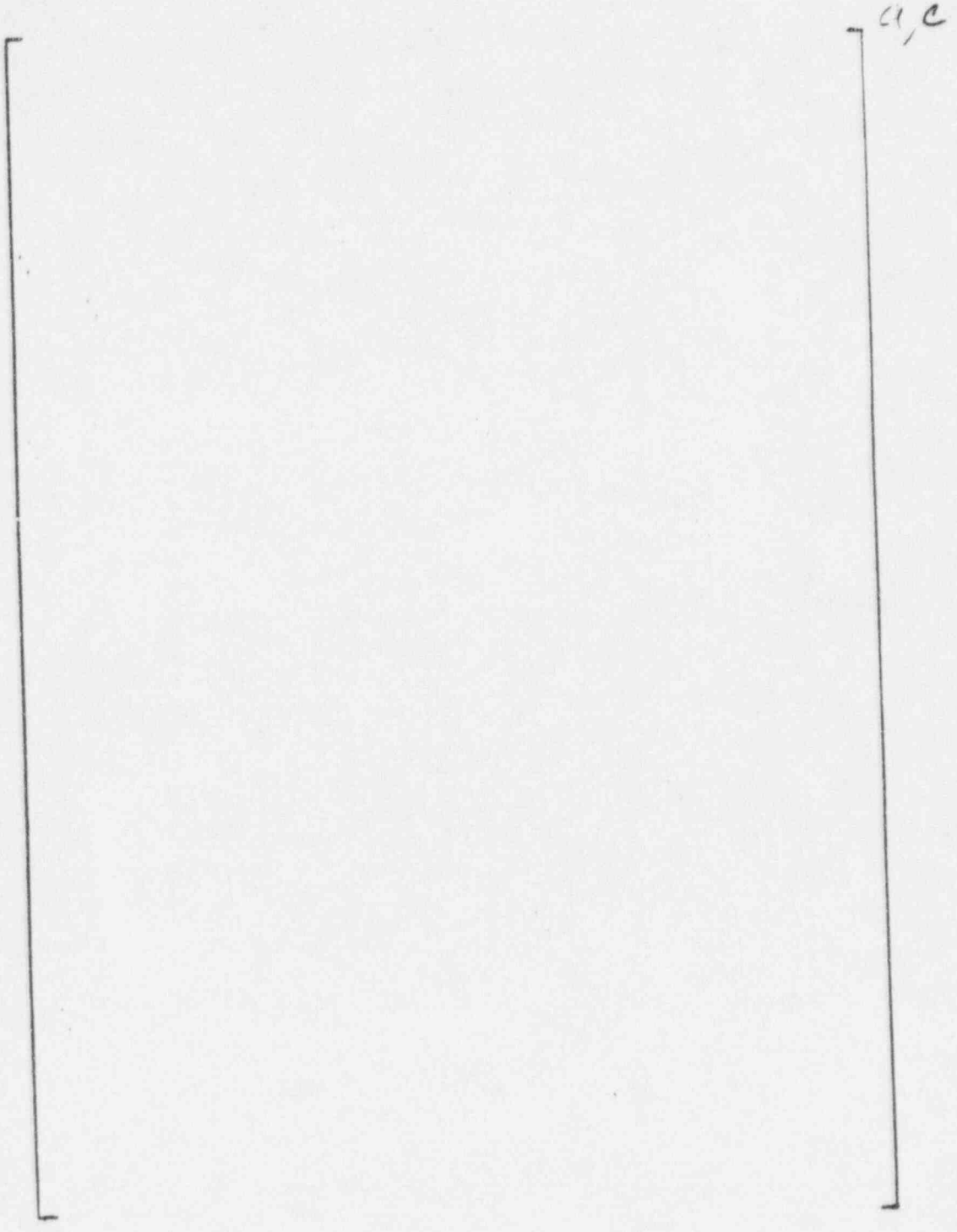

Figure 8-1 - Phase 3 Water Distribution Test Coverage as a Function of Flow Rate

8.2.3 STC Wet Flat Plate Tests

The primary purpose of the STC wet flat plate tests was to generate heat and mass transfer data for evaporative cooling with parameters that bound the expected conditions on the AP600 containment shell. A secondary purpose was to observe the film hydrodynamics including possible formation of dry patches due to surface tension instabilities.

Tests were performed in 2 orientations; vertical (to represent the sidewall) and 15 degrees from horizontal (to represent the upper portion of the dome) with various combinations of air velocity, film flow rate and heat flux. A stable, wavy laminar water film was formed easily on the hot coated steel surface, even in the vertical orientation. A description of the test section and results from the various tests are given in Ref. 8.3. The test data are summarized in Table 8-3.

Two of the heated flat plate tests were run with very low film flow rates at relatively high heat flux (6000 - 8000 BTU/hr-ft^2) to force the film to dryout before reaching the end of the test section. The observations are given in Ref. 8.3 (pages 36-37). "The upper part was 80% wetted and fingers of water film extended down four feet to within two feet of the end of the heated plate. The bottom of the fingers slowly moved up and down. The dry patch between fingers was between one quarter of an inch and one and one half inches wide. These tests showed that the end point of water films on the containment would still be stable film evaporation, even with very thin films and high heat fluxes."

8.2.4 Small Scale Tests

The small scale tests were designed to provide heat and mass transfer data for both the inside and outside of the test vessel. The test apparatus consisted of a 3-ft. diameter, 24-ft. high steel pressure vessel that was heated by steam supplied at various pressures. The pressure vessel was surrounded by a clear, plexiglass shield that formed a 15-in. wide annulus for either forced or natural circulation driven air flow and allowed observation of the applied external film flow.

The tests were conducted with varying steam supply flow rates, water film flow rates, water film temperatures, inlet air flow rates, inlet air temperature and humidity. Instrumentation was provided to measure internal steam condensation rates, external water evaporation rates, inner and outer wall temperatures, film temperatures, air velocity, temperatures and humidity. A summary of the test data from Ref. 8.4 (for tests with measured water coverage) is provided in Table 8-4.

The following observations and conclusions (with respect to the water film) were drawn from these tests:

- A stable, uniform, wavy laminar film was formed on the inorganic zinc coated steel surface using simple weirs.

- The film remained stable and uniform on the vertical sidewall of the vessel at average, evaporating heat fluxes in the range of those expected on the AP600.

a,c

[ ] 9,c

Table 8-1 Summary of Small Scale Tests

8.2.5 Large Scale Tests

The Westinghouse large scale PCS test facility was built to provide heat and mass transfer test data for a geometrically similar model of the AP600 containment vessel. The tests provided experimental data that was used for evaluating the physics in containment, determining the relative importance of various parameters that affect heat and mass transfer and validating computer codes or models. Three series of tests were run at the Westinghouse large scale PCS test facility. The steady-state pressure, annulus air flow rate, water flow rate, steam flow rate, injection velocity, location and orientation, and noncondensible gas concentration were varied between the tests. Test conditions were selected to provide heat and mass transfer validation over a range of post-accident containment operating conditions for the AP600.

The large scale PCS test facility uses a 20-ft. tall, 15-ft. diameter pressure vessel to simulate the AP600 containment vessel. The geometry is approximately a 1/8-scale of the AP600 containment vessel. A plexiglas cylinder is installed around the vessel to form the air cooling annulus. Air flows upward through the annulus via natural convection to cool the vessel, resulting in condensation of the steam inside the vessel. A fan is located at the top of the annulus shell to provide the capability to induce higher air velocities than can be achieved during purely natural convection. Water is applied to the elliptical dome surface by two rings of J-tubes. This method of application produces a series of uniformly spaced stripes which provide evaporative cooling. A typical stripe flow pattern is shown in Figure 8-2.

Evaporation and spreading due to the area divergence on the inclined surface of the dome caused the thickness of the stripes to decrease as the width (wetted perimeter) increased. At low heat fluxes and water flow rates scaled to the initial PCS flow rate on the AP600, the stripes spread within a few inches of their application point to form a continuous wavy laminar film. At higher heat fluxes or lower scaled PCS flow rates, some of the individual film stripes became unstable and dry spots formed just below, and in line with, the J-tube location (as shown in Figure 8-2). In this case, the film stripes did not spread to complete circumferential coverage.

The following important observations (with respect to film coverage) were made during the tests:

- The individual film stripe widths were observed to remain relatively constant as the film flowed down the vertical sidewall.

- The film stripes remained stable (i.e. they did not split or bunch up) as they evaporated on the vertical sidewall.

- No dry patches, other than those in line with a source, were observed.

These observations indicate that evaporating film stripes on the vertical sidewall are more stable than a diverging subcooled film on top of the dome.

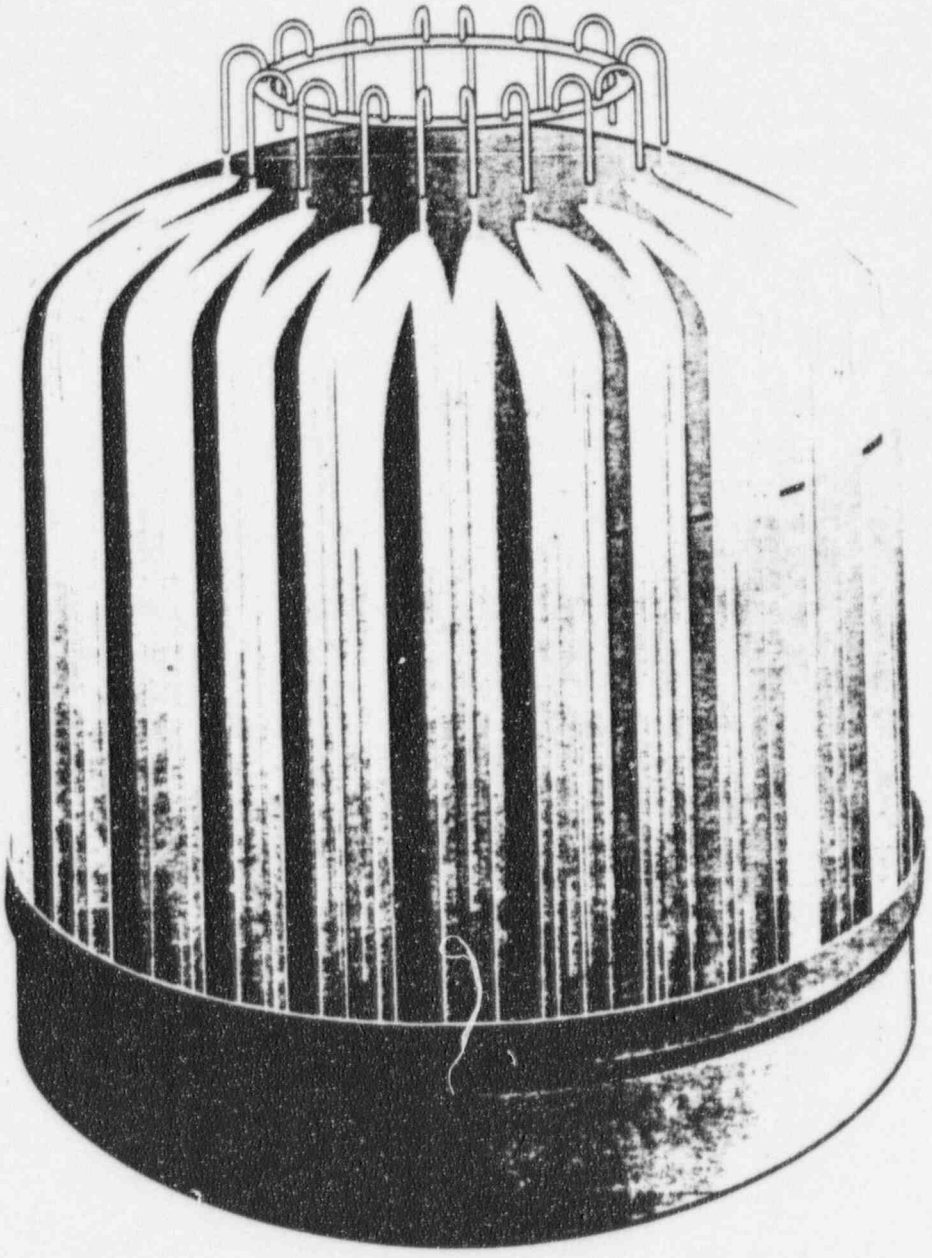

Figure 8-2 - Large Scale Test Water Coverage Pattern

An evaluation of the large scale test data (Ref. 8.5) yielded some additional important conclusions with respect to film coverage and heat removal:

- Evaporation was the primary mode of heat removal from the outside of the vessel (approximately 75 percent of the total), followed by sensible heating of the subcooled liquid film (approximately 17 percent of the total). The remainder of the heat was transferred to the environment by convection and radiation.

- For the same wetted perimeter, striped film coverage provided better heat removal than forced quadrant coverage.

- For all of the wetted large scale tests (except the horizontal, high velocity steam jet injection case), the highest heat flux occurred near the top of the dome at the elevation where the external film was applied. Although the dome represents about 30 percent of the heat transfer surface area, approximately 40 percent of the total heat removal occurred on the dome and 60 percent on the cylindrical sidewalls.

- Injection of high-velocity steam (similar to a steamline break) resulted in a well mixed vessel (both above and below the operating deck), and thus a relatively uniform wall temperature and heat flux over the evaporating surface.

The Baseline and Phase 2 test data related to water coverage from Ref. 8.6 and Ref. 8.7 (excluding the tests with forced water coverage) is summarized in Table 8-5. This data is used to bound the film stability model as described in Section 8.4.3.

-a,c

Table 8-5 Summary of Large Scale Tests

8.2.6 Estimated AP600 Range of Film Coverage Parameters

The estimates for the maximum and minimum values for the range of AP600 film coverage parameters during a DBA are calculated using the simple approach described below. The AP600 range of film coverage parameters is compared with the range of the PCS tests.

A conservative estimate for the gravity driven PCS water flow rate is calculated assuming a single failure of 1 of 2 valves (located in parallel) to open. This flow rate is shown in Figure 8-3. A combination of 3 standpipes is used along with orifices to adjust the delivered flow rate with time. The flow rate is adjusted based on decay heat removal requirements. Note, the largest flow resistance is in the orifices, so the single failure assumption reduces the gravity driven flow rate by less than 2 percent. The flow rate decreases with time as the water level in the PCS storage tank decreases. The 2 large decreases in flow rate (at about 5 and 20 hours) occur when the water level falls below the first and second standpipes. The minimum PCS flow rate occurs after about 3 days. Values of 220 gpm and 55 gpm are used for the maximum and minimum PCS flow rates in the calculations below.

The minimum sidewall film flow rate, Γ, would be 0 lbm/hr-ft. To determine a maximum sidewall Γ, only 25% of the film is assumed to evaporate on the dome. It is likely that there would be more evaporation from the dome, which would reduce the film flow rate to the sidewall. With a 25% reduction in the PCS flow to the sidewall, measurements from the unheated, phase 3 Water Distribution Tests indicate that approximately 75% of the perimeter at the top of the sidewall will be wetted, resulting in an estimated maximum sidewall film flow rate of 256 lbm/hr-ft. At the estimated maximum 200°F film temperature, the sidewall Re_{film} would be 1400. The Re_{film} and Γ values on the dome will be higher than the sidewall values since Γ decreases as the diameter increases. A more detailed comparison of the expected AP600 Re_{film} value with test data is given in Ref. 8.8.

The internal shell heat flux provides the boundary conditions for the evaporating film. Condensation is the primary source of energy transfer to the internal surface of the shell. The condensation rate is dependent on the internal gas velocity along the shell, the internal steam distribution and the internal shell temperature. Large-scale test data indicate that the volume above the operating deck will be well mixed by the high velocity break jet during a MSLB event and the early blowdown phase of a LOCA event, but will be stably stratified (i.e. a vertical, density gradient will form) during the post-blowdown portion of a LOCA event. The shell temperature is highest in locations where the exterior surface is dry.

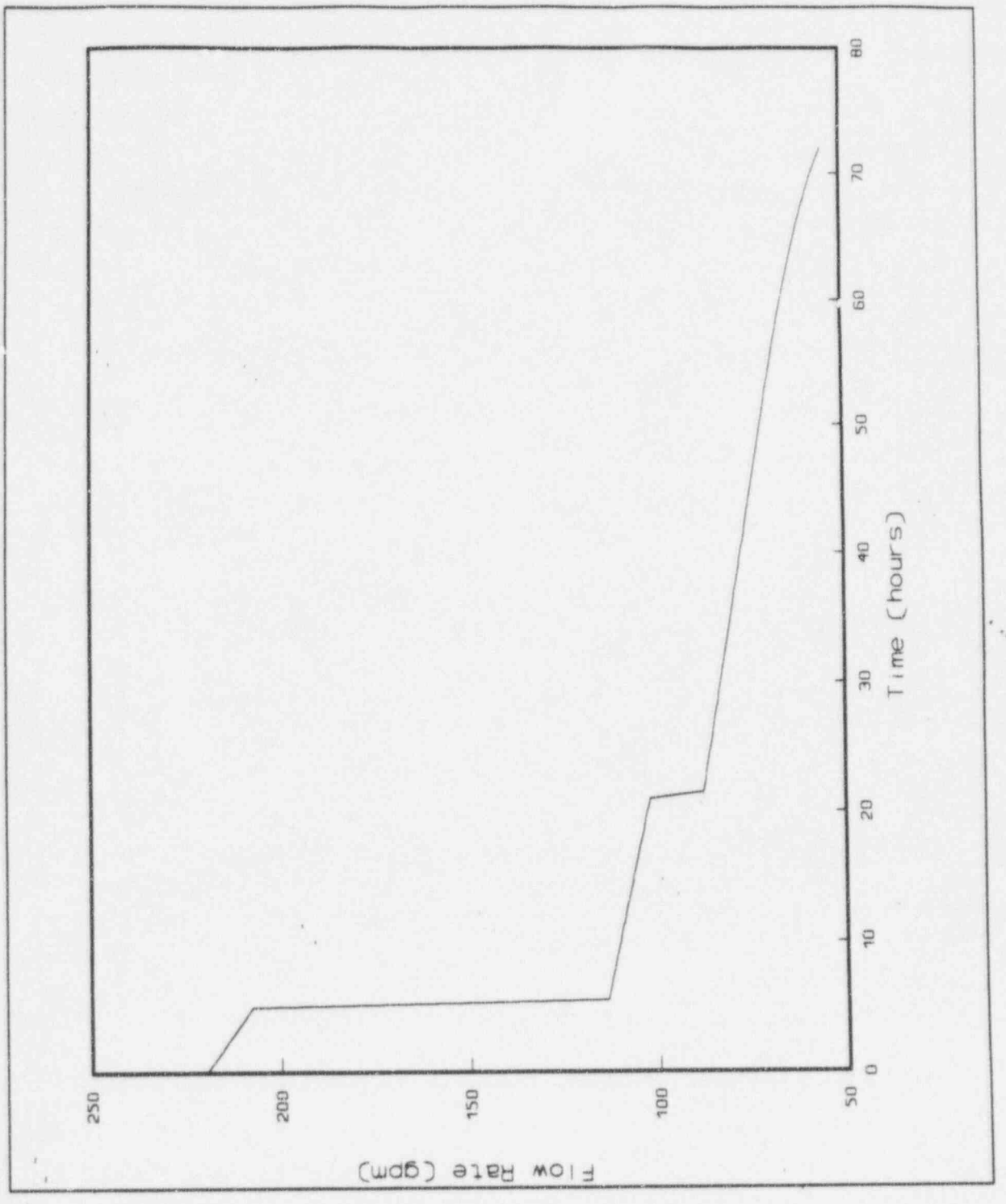

Figure 8-3 - Conservative Estimate of the Gravity Driven PCS Flow Rate

The steady state shell average heat flux and film temperature were calculated for the subcooled, evaporating and dry portions of the shell assuming an initial ambient air and film temperature of 120°F. These calculations were performed at the containment design pressure, 45 psig, to bound conditions at the expected DBA peak pressure and at 22.5 psig, for conditions representative of 24 hours after blowdown. The results are tabulated below.

Containment Pressure (psig)	Avg. Subcooled Heat Flux (BTU/hr-ft^2)	Avg. Subcooled Temp. (°F)	Avg. Evaporating Heat Flux (BTU/hr-ft^2)	Avg. Evaporating Temp. (°F)	Avg. Dry Heat Flux (BTU/hr-ft^2)	Avg. Dry Temp. (°F)
45	7740	155	5500	190	455	260
22.5	3700	147	2500	175	300	220

The maximum wet shell heat flux is estimated to be 50% higher than the average subcooled value (at 45 psig); this would be about 11500 BTU/hr-ft^2. The minimum wet shell heat flux is estimated to be at least 50% lower than the average evaporating value (at 22.5 psig); this would be about 1300 BTU/hr-ft^2.

Per the Technical Specifications, the initial PCS film temperature will be between 50 and 120°F. The 120°F value is used in the DBA evaluation model to minimize the benefit of sensible heat removal by the subcooled film. The film temperature will increase as the film flows down the dome and onto the sidewall. The maximum evaporating film temperature was estimated to be less than 200°F. Since the resistance to heat transfer through the thin film is very small (compared with the mass transfer and internal resistance, as shown in Ref. 8.9) and the heat flux is relatively low, the maximum wet shell surface temperature is estimated to be less than 20°F higher than the maximum film temperature.

The estimated range of the AP600 film parameters during a DBA is summarized in Table 8-6. A comparison with the PCS test data range shows that, with the exception of the maximum evaporating film temperature and maximum sidewall Re_{film} number, the test data bounds the estimated range of the AP600 film parameters.

Table 8-6 - Comparison of the Range of Film Coverage Parameters

a,c

[ ]

The test data parameter ranges are sufficient for evaluating the film stability model even though the estimated maximum film temperature and maximum Re_{film} are not covered. It is more important to cover the lower expected film temperature with the test data, than the higher expected film temperature since the film is less stable at lower film temperatures. Also, it is more important for the tests to cover the minimum sidewall Re_{film} for evaluating the film stability model. Also note, the test data for the maximum sidewall Re_{film} number is within the wavy laminar flow regime, while the maximum AP600 sidewall value is in the transition to turbulent flow regime. The resistance to heat transfer through the film is lower in the turbulent flow regime than in the laminar flow regime, so even though the tests did not cover the transition regime, the test results are conservative with respect to evaluating the resistance to heat transfer.

8.3 AP600 Transient Wetting Behavior

Water begins to flow onto the top of the AP600 containment vessel shortly after the PCS actuation signal occurs. The time sequence of events to establish steady state water coverage of the AP600 following actuation of the PCS is shown in Table 8-7 below.

Table 8-7 PCS Time Sequence of Events

Event	Time (sec)
Signal Actuation	0
Valve Strokes Open	20
Piping Fills	50
Bucket Fills & Spills	53
First Weir Fills & Spills	203
Second Weir Fills & Spills	353
Steady State Established	653

The maximum time for water to begin flowing onto the shell surface, following a postulated event that actuates the PCS, is 53 seconds and is based on a maximum 20 second valve stroke time plus 30 seconds to fill the pipes and 3 seconds to fill the bucket.

The Water Distribution Tests (described earlier) were used to test the ability of various weir designs to cover a large fraction of the containment shell with water and to determine the time to establish steady state film coverage on the AP600. Based on a review of the video tapes of the phase 3 (improved weir design) Water Distribution Tests, the time to fill and begin to spill over the first weir with a flow rate of 27.5 gpm (equivalent to the single valve failure flow rate of 220 gpm on AP600) was conservatively estimated to be about 2.5 minutes; the time to fill and begin to spill over the second weir was conservatively estimated to be about 5 minutes; and the total time to establish steady state coverage of the dome and sidewall was estimated to be about 10 minutes.

The shell surface temperature continues to increase during the period to establish steady state coverage. The time for the dry outer shell to reach a given temperature is a function of the internal containment air temperature, the internal energy transfer coefficient and the shell thickness. It can be calculated using the properties of the [ ]^{a,c} steel shell and Figure 4-8 from Kreith (Ref. 8.10).

The initial shell temperature is assumed to be 120°F. The time for the dry external shell surface temperature to reach the boiling point (212°F) can be calculated with the following input:

T = 212°F (external shell surface temperature)
T_i = 120°F (initial shell temperature)
T_∞ = 250°F (internal containment air temperature)

$\zeta = (T - T_\infty)/(T_i - T_\infty) = 0.292$

The properties of the steel shell are given below:

k_s	= 25 BTU/hr-ft-F	(thermal conductivity)
L	= [ ]^{a,c} ft	(thickness)
α	= 0.49 ft^2/hr	(thermal diffusivity)

If the internal energy transfer coefficient (primarily condensation in air) is assumed to be much larger than the external energy transfer coefficient (primarily forced convection) such that the dry outer shell surface can be considered adiabatic (insulated) over the time period of interest, then the time to reach 212°F will be minimized. The results of the calculation are tabulated as a function of the internal energy transfer coefficient below:

U (BTU/hr-ft^2-F)	1/Bi	$\alpha t/L^2$	t (seconds)
5	34.3	43	5792
10	17.1	22	2963
50	3.43	5	673
100	1.71	2.6	350

The average, internal energy transfer coefficient for AP600 following a DBA LOCA is estimated to be about 75 BTU/hr-ft^2-F, therefore, the time for the dry outer containment shell temperature to reach the boiling point is estimated to be between 400 and 600 seconds.

A WGOTHIC AP600 model was run for comparison with the hand calculations. The calculated temperatures at the top of the dome, before application of the PCS film, are shown in Figure 8-4. Figure 8-5 shows that condensation provides the bulk of the internal energy transfer to the shell. During the 10 minute transient time after the initial blowdown, the containment temperature (and therefore the maximum possible internal shell temperature) is maintained at about 260°F by condensation on the heat sinks inside containment. The WGOTHIC calculation of the time for the shell surface temperature on top of the dome to reach 212°F (about 450 seconds) agrees reasonably well with the estimate above. The heatup rate is about 0.2°F/sec and falls between the 50 and 100 BTU/hr-ft^2-F internal energy transfer coefficient values assumed in the hand calculation.

The calculated temperature increase in the dry external shell surface is shown as a function of time in Table 8-8 below.

Table 8-8

Event	Time (sec)	Increase in Dry, External Shell Temp. (F)
Signal Actuation	0	0
Valve Strokes Open	20	
Piping Fills	50	
Bucket Fills & Spills	53	10
First Weir Fills & Spills	203	50
Second Weir Fills & Spills	353	70
Steady State Established	653	120

At the maximum time delay for water application to the shell (53 seconds, from Table 8-7), the outer shell temperature will have increased by less than 10°F. The temperature of the dry portion of the outer shell will have increased by less than 50°F at the time the first weir begins to spill (about 203 seconds) and less than 70°F at the time the second weir begins to spill (about 353 seconds). Therefore, the sidewall temperature will be less than 200°F at the time the stripes of water film begin to advance down the vertical surface. The outer shell surface temperature for the dry regions of the dome and sidewall will not exceed 240°F before steady state water coverage is established.

Water coverage is not adversely affected by application of the film to a hot, dry shell surface. Tests run during the PCS testing program verified the ability of the water film to wet and rewet a hot, dry surface (temperature exceeding 240°F) coated with the inorganic zinc compound. Video tapes of the STC wet flat plate show the initial wetting, dryout and re-wetting of a hot, dry plate in both a vertical and inclined position. The dry plate temperature was estimated to be about 240°F (based on the maximum heating fluid temperature). An applied wavy laminar film quickly covered the hot, dry plate. As the flow rate was reduced, the waves in the film became smaller and eventually disappeared. The plate remained visibly wet until after the film flow was turned off, then dry patches appeared and grew in circumference as the plate dried out. Video tapes also show the initial wetting of the large-scale test vessel. The measured shell surface temperature was about 260°F at the time the water was applied. The film front was observed to "sizzle" as it quickly advanced downward and covered the surface of the elliptical dome.

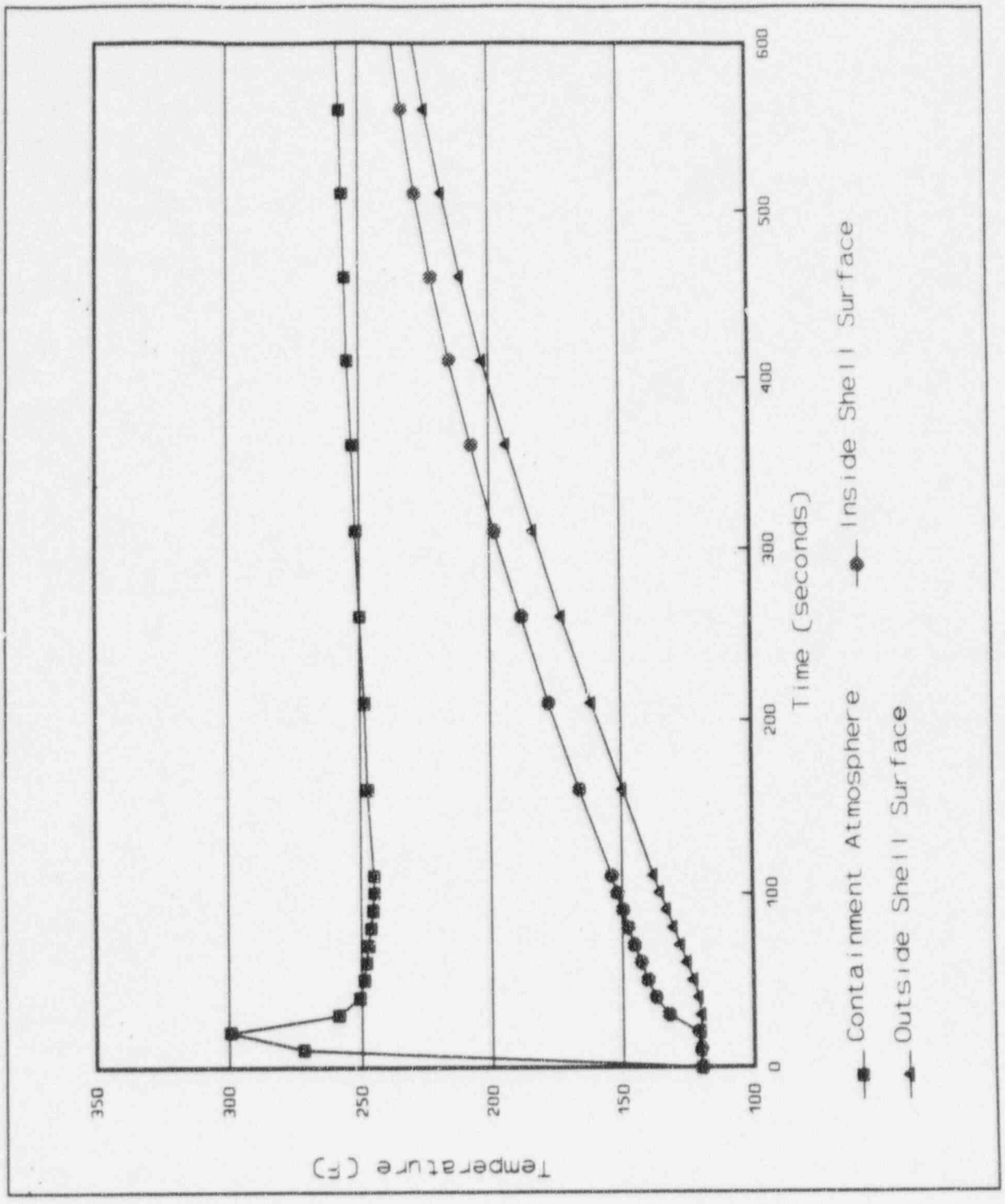

Figure 8-4 - Shell Temperatures at the Top of the Dome (without PCS Film Flow)

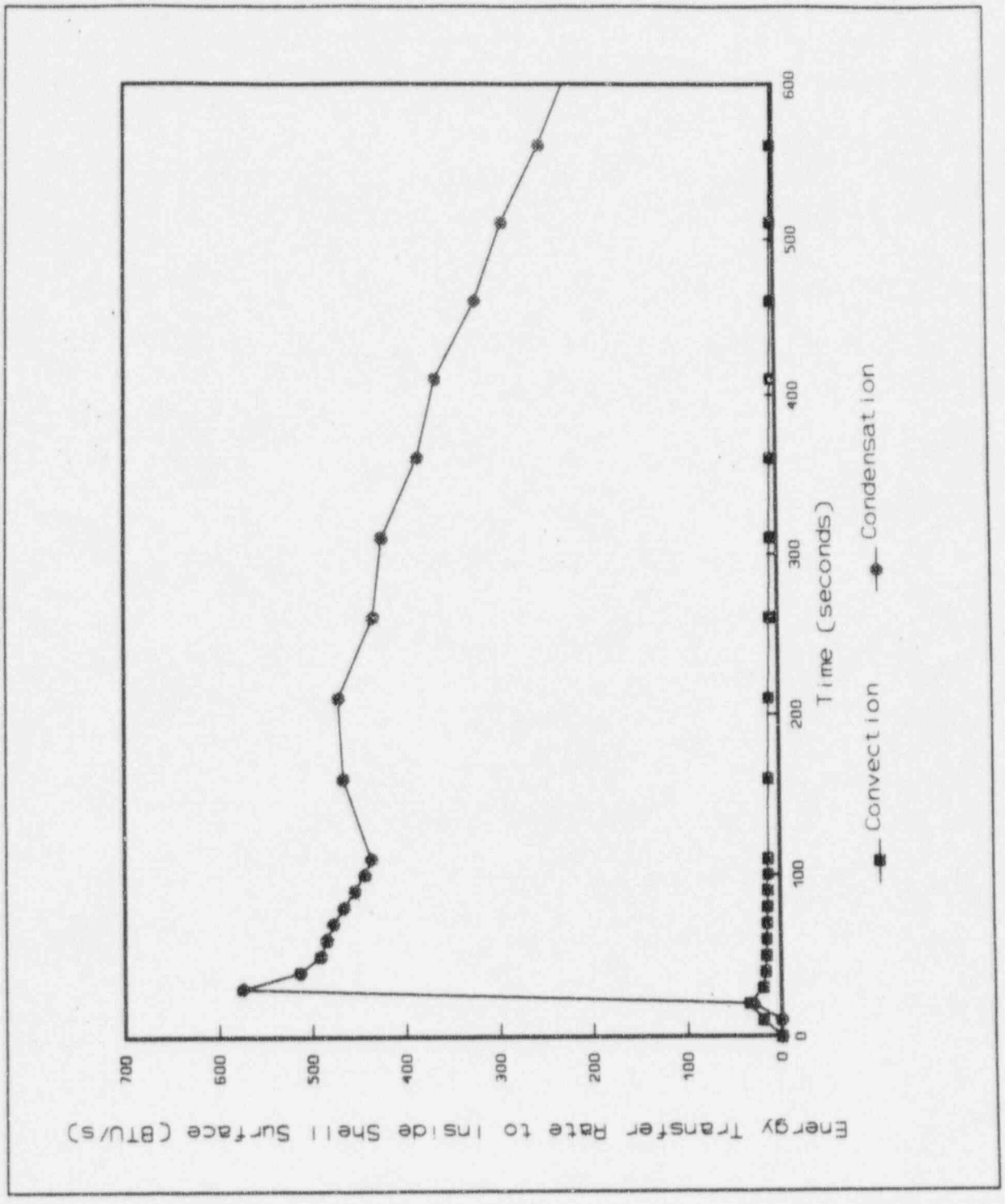

Figure 8-5 - Comparison of Internal Condensation and Convective Energy Transfer at the Top of The Dome

8.4 Analytical Model for Determining Film Stability

The stability of liquid films has attracted the attention of many analysts and experimenters over the last 40 years and has been examined from two different points of view: looking at the minimum flow rate required to re-wet a stable dry patch, or looking at the thermocapillary breakdown of the thin film. Norman and McIntyre (Ref. 8.11) presented data that showed a large increase in the minimum film wetting rate was required as the temperature difference between the surface and film was increased. Hallett (Ref. 8.12) also observed this phenomena and developed a film breakdown correlation that was related to the film surface tension difference, the wave number and the heat transfer coefficient. Fujita and Ueda (Ref. 8.13) measured the breakdown of both subcooled and saturated liquid films on heated, vertical, polished, stainless steel tubes. A comparison of the results from their tests also showed that the highly subcooled films become unstable at flow rates several times higher than saturated films. More recently, Bohn and Davis (Ref. 8.14) also measured the breakdown of subcooled water films on heated, vertical, polished, stainless steel tubes and developed a film breakdown correlation that was dependent on thermocapillary effects.

Subcooled films, with temperatures much lower than the solid surface temperature, absorb heat causing the film temperature to increase. Evaporating films, that are more nearly in thermal equilibrium with the solid surface, transfer mass and energy from the film surface to the gas atmosphere. An apparent explanation for the reduced stability of subcooled films is the existence of significantly higher temperature gradients that give rise to increased thermocapillary forces.

The list of papers considered for application to AP600 is extensive and will not be given here. However, in a summary article (Ref. 8.15), Bankoff provided an extensive list of relevant papers, many of which have been considered for application to AP600. The current state of the art is focused on the "moving contact line", which was also considered for application to AP600, but is generally not very practical for engineering application. Overall, investigators have identified momentum, surface tension, thermocapillary, and vapor thrust as the dominant forces affecting film stability. These forces are typically expressed as functions of flow rate, heat flux, fluid properties, and wetting angle. Vapor thrust can be neglected in AP600 because the heat flux is low, less than 10,000 BTU/hr-ft^2. Consequently, for AP600, it is necessary to address momentum, surface tension, and thermocapillary forces.

The model selected to perform AP600 film stability calculations was developed by Zuber and Staub (Ref. 8.16) to predict the conditions under which a stable dry patch will form. Since this model relies on local film and surface conditions, it is applicable to any size structure.

The Zuber-Staub model considers the stability of a dry patch located within a uniform, flowing film, i.e. the inability of the liquid film to recover the dry patch. The Zuber-Staub model uses a vertical force balance at the tip of a postulated dry patch to determine the minimum uniform film thickness required to rewet the dry patch. This minimum film thickness is a function of the surface heat flux, the film properties (including the contact angle between the film and surface), and the surface inclination angle.

According to the Zuber-Staub model, if the uniform film thickness were greater than the minimum stability value, any dry patch created in the film would be washed over and would readily disappear after formation due to the momentum of the flowing film. Conversely, if the film thickness were equal to or less than the minimum stability value, a dry patch, if formed, would be predicted to be stable, i.e. the uniform film would not be able to recover the dry patch. The Zuber-Staub model does not consider the effects of waves in recovering the dry patch.

A modified form of the Zuber-Staub model (shown below) was selected for AP600 because it includes each of the dominant terms: momentum, surface tension, and thermocapillary.

$$\frac{\rho^3(g\sin\beta)^2\delta^4}{15\mu^2} + \rho g\cos\beta\frac{\delta}{2} = \frac{\sigma}{\delta}(1-\cos\theta) + \frac{d\sigma}{dT}\frac{q''}{k}\cos\theta$$

where:
- θ = the contact angle between the surface and film
- β = the surface angle of inclination relative to horizontal
- σ = the liquid surface tension
- $d\sigma/dT$ = the liquid surface tension temperature derivative
- q'' = the surface heat flux
- k = the liquid thermal conductivity
- ρ = the liquid density
- μ = the liquid viscosity
- g = the gravitational constant
- δ = the minimum stable film thickness

A body force term was added to account for spreading on the inclined surface of the elliptical dome and the vapor thrust term was eliminated.

8.4.1 AP600 Film Stability Model Sensitivities

The mass flow rate per unit perimeter, Γ, is more easily measured than the film thickness. The average film thickness in laminar film flow is related to Γ as follows:

$$\delta = \left[\frac{3\Gamma\mu}{g\sin\beta\,\rho^2}\right]^{1/3}$$

The sensitivity of the predicted Γ_{min} value to the contact angle and film temperature is shown as a function of heat flux in Figures 8-6 and 8-7 (for film temperatures of 120 and 200°F respectively). Γ_{min} decreases with increasing film temperature, consistent with test observations. At very small contact angles, Γ_{min} increases as the heat flux increases. At larger contact angles ($\theta > 10°$), Γ_{min} is not very sensitive to the estimated AP600 heat flux range during a DBA.

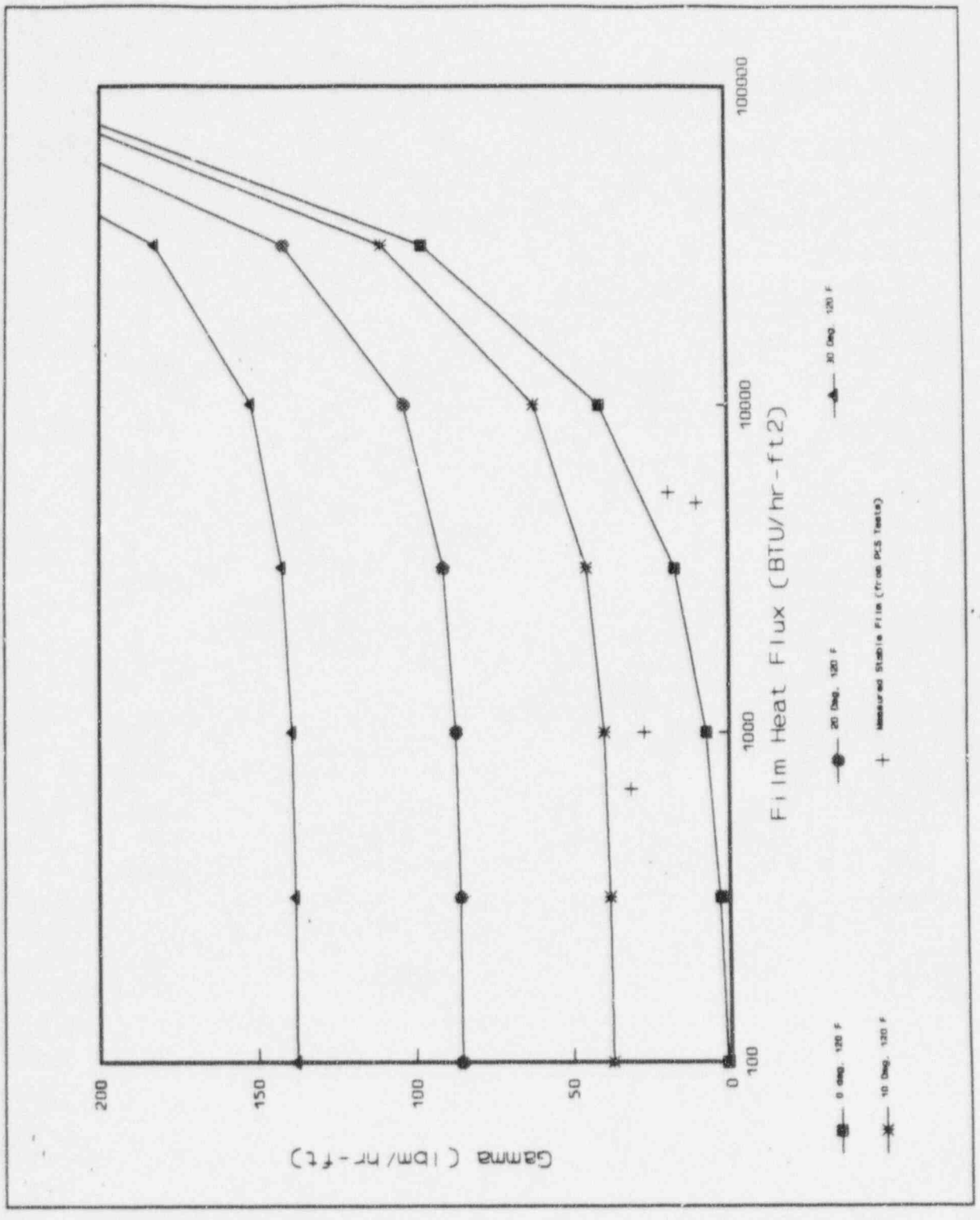

Figure 8-6 - Minimum Stable Film Flow Rates Predicted by the Modified Zuber-Staub Model Showing Sensitivity to Heat Flux and Wetting Angle at 120°F Film Temperature

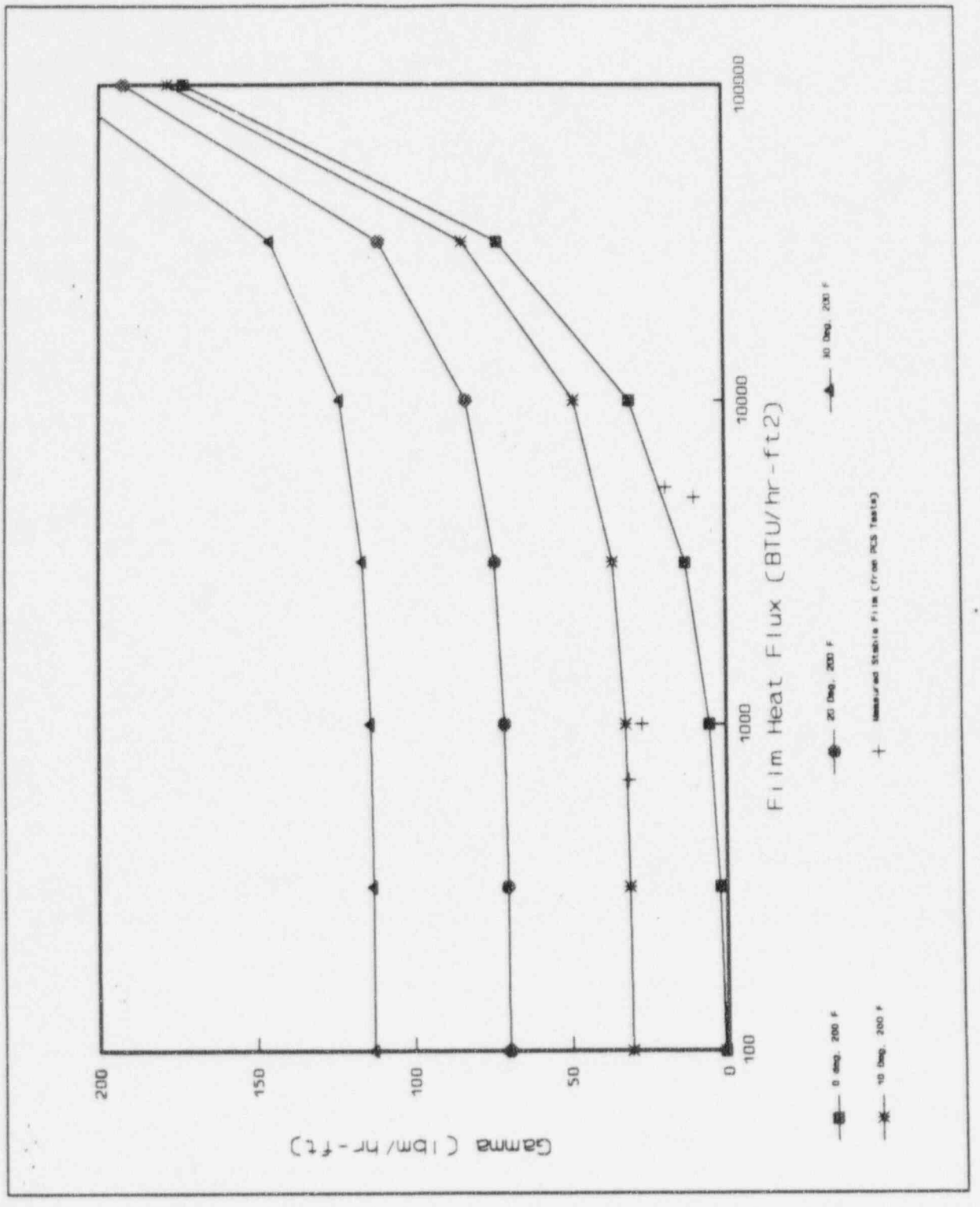

Figure 8-7 - Minimum Stable Film Flow Rates Predicted by the Modified Zuber-Staub Model Showing Sensitivity to Heat Flux and Wetting Angle at 200°F Film Temperature

8.4.2 Contact Angle and Surface Wettability

The contact angle between a water film and the surface is an important input to the AP600 film stability model. The contact angle is an indication of the surface wettability. Better wetting occurs on surfaces with small contact angles. Contact angles are measured for both advancing and receding films and usually the two values are quite different with the advancing contact angle being much larger than the receding contact angle.

The AP600 containment shell surface will be coated with an inorganic zinc compound for corrosion protection. The contact angle for a slowly advancing drop of water was measured as a function of temperature and age of the surface. These results are presented in Ref. 8-17 and show the advancing contact angle for this surface decreases with age and temperature, and is between [ ]^{a,c} for a new surface, and between [ ]^{a,c} after just 2 years of weathering. An advancing contact angle value of [ ]^{a,c} was chosen for the film stability calculations because it is the upper bound of the measured, steady state values for a heated, weathered surface.

A small drop of water spread around on the inorganic zinc coated surface does not contract, or snap back into a drop, demonstrating that the receding contact angle is nearly zero. Because the receding wetting angle is nearly zero, the film is expected to flow in constant width stripes down from the vessel springline (top of the vertical cylinder). This is consistent with observations of the film behavior on the Large Scale Tests discussed earlier. From another point of view, these observations imply that the film breakdown to form a dry spot occurs at a lower film Reynolds number than the critical Reynolds number for rewetting. This is not surprising, since the contact angle formed in enlarging a small dry spot is smaller (~0) than in rewetting it.

A solid surface will be wet with liquid if the free surface energy of the solid is greater than the surface tension of the liquid. Surface tension, σ, is defined as the work required to expand the surface of a liquid by a unit of area. It is a measure of the strength of the intermolecular forces in the fluid, similar to the latent heat of vaporization.

Hydrogen bonding is the strongest type of intermolecular force. Liquid water has relatively strong intermolecular forces due to the strong hydrogen bonds; 80% of the intermolecular attraction in water is attributed to hydrogen bonding. In a water molecule, the electrons spend more time in the vicinity of the oxygen atom than the hydrogen atoms because oxygen is more electro-negative than hydrogen (3.5 vs. 2.1 for hydrogen on a scale of 4.0). This results in an electric dipole within the molecule. For this reason water is said to be a polar molecule.

As temperature increases, the mean spacing between molecules in a liquid increases causing the density to decrease and a reduction in the intermolecular forces. Therefore, both σ and the latent heat of vaporization decrease with increasing temperature. For example, the surface tension of water is about 4.97E-03 lbf/ft and the latent heat of vaporization is about 1054 BTU/lbm at room temperature. These decrease to 4.0E-03 lbf/ft and 970 BTU/lbm respectively at 212°F.

The wetting of a solid surface by water is improved by reducing the surface tension of the water (by use of a wetting agent, such as a detergent) or by making the surface more porous (to improve the spreading by capillary action). The porosity of the inorganic zinc coating is believed to be the primary factor affecting wetting early in life. It was postulated that the buildup of polar molecules (e.g., oxides of Zn) on the surface improved the wetting with age. Tests on both new and weathered surface coating samples were performed using a scanning electron microscope with an energy dispersive X-ray spectrometer to identify the chemical species present on the surface. More oxides of zinc were found on the weathered surface, supporting the hypothesis that the increase in wetting is due to the surface becoming more polar as it ages.

Buildup of some surface contaminants can result in a reduction in wettability. The worst surface contaminant is silicone because it has a very low surface energy and low polarity. Other surface contaminants, that could result in reduced wetting, include hydrocarbons; i.e. oils, members of the PTFE family (Teflon), polypropylene and polyethylene residues. The coatings vendor has a standard cleaning procedure and a specially developed detergent available that emulsifies these types of surface contaminants so they can be washed away.

Although the number of potential contaminants that would adversely affect wetting is probably limited to a dozen or so, it would be very difficult to analytically predict the wetting degradation over time. We would have to estimate the degradation of surface wettablility as a function of the concentration of each, the deposition rate of each as a function of the local or worst case atmospheric conditions, assume the degradation is additive, etc. Therefore, periodic In-Service Inspections will be performed to sample the surface for wettability. The frequency and procedures for testing and the minimum acceptance criteria prior to cleaning the surface are defined in the Reliability Assurance Program.

8.4.3 Comparison of the AP600 Film Stability Model with Test Data

The PCS tests provided measurements of film flow rates on the prototypical AP600 surface. Stable, evaporating films were produced in the STC wet flat plate tests and the small-scale tests. Subcooled film breakdown was observed to occur just below the J-tube location on the dome in some of the large-scale tests, as described in Section 8.2.5, but the evaporating film stripes that traveled down the vertical sidewall remained stable and maintained a relatively constant width. A compilation of the film data from these 3 tests is provided in Tables 8-3, 8-4 and 8-5.

The lowest measured film flow rates from the PCS tests are shown in Figures 8-6 and 8-7 for comparison with the modified Zuber-Staub film stability model calculations. Note, these data points represent stable, evaporating films on the vertical, prototypical surface. These measured film flow rates are significantly lower than the predicted stability limit calculated with the model (using a measured contact angle of [ ]^{a,c}). Therefore, the modified Zuber-Staub film stability model will over-predict the breakdown flow rate of evaporating films on the vertical sidewall of the AP600 containment.

The breakdown of subcooled films was observed on the prototypical surface in some of the large-scale tests, but it was not accurately measured. The heat flux and film flow rate at the point of breakdown were estimated using the measured data on the top of the dome.

The estimated film Re number at breakdown is shown as a function of the maximum dome heat flux in Figure 8-8. For comparison, minimum stable film Re number curves are calculated using both the modified Zuber-Staub film stability model and the AP600 film stability model with a [ ]^{a,c} advancing contact angle, an estimated surface inclination angle (at the breakdown location) of 20° and an estimated film temperature (at the breakdown location) of 80°F. Note, as described later in this section, the AP600 film stability model includes a multiplier for subcooled film breakdown that bounds all of the PCS test data. The estimated film Re number at breakdown is, in most cases, higher than the predicted stability limit calculated by the modified Zuber-Staub model. The AP600 film stability model bounds the breakdown flow rate of subcooled films on the prototypical surface.

The modified Zuber-Staub film stability model was compared with published subcooled film breakdown data on other surfaces. Fujita and Ueda (Ref. 8.13) and Bohn and Davis (Ref. 8.14) measured the breakdown of subcooled water films on heated, vertical, polished, stainless steel tubes. A wide range of film flow rates and heat fluxes was covered; the subcooled film temperatures were between 70 and 170°F. The minimum stable film Re number calculated by the AP600 film stability model, using a 65° advancing contact angle for stainless steel (Ref. 8.18), was compared with this data set. The results are shown in Figure 8-9.

A comparison of the range of subcooled film Re numbers at breakdown between the polished, vertical, stainless steel tube surface and the prototypical inorganic zinc coated surface (Figures 8-8 and 8-9) shows that the subcooled film remains stable at much lower flow rates on the inorganic zinc coated surface over the same range of heat fluxes. The stainless steel and copper surfaces, typically used in film stability studies, do not wet well and consequently are expected to exhibit less stable films than the inorganic zinc coating on the AP600 containment shell. Therefore, it is important and appropriate to use film stability data from the prototypic surface to validate the AP600 film stability model.

All three data sets show the modified Zuber-Staub film stability model is relatively insensitive to heat flux in the range of the subcooled film test data. At higher heat fluxes, the model predicts stable dry patches will be formed at lower Re numbers than were measured in the tests; and at lower heat fluxes, the model predicts stable dry patches will be formed at higher Re number than were measured in the tests.

It is quite clear that the modified Zuber-Staub film stability model does not predict the subcooled film breakdown data for either the prototypical surface or the stainless steel tubes. One approach to force the model to better correlate the subcooled film breakdown data is to apply a multiplier to the thermocapillary term in the model. Another approach is to apply a multiplier to the prediction of the minimum stable subcooled film flow rate and bound all of the test data from the prototypical surface over the entire heat flux range of interest. This second, more conservative, approach has been chosen for the AP600 film stability model.

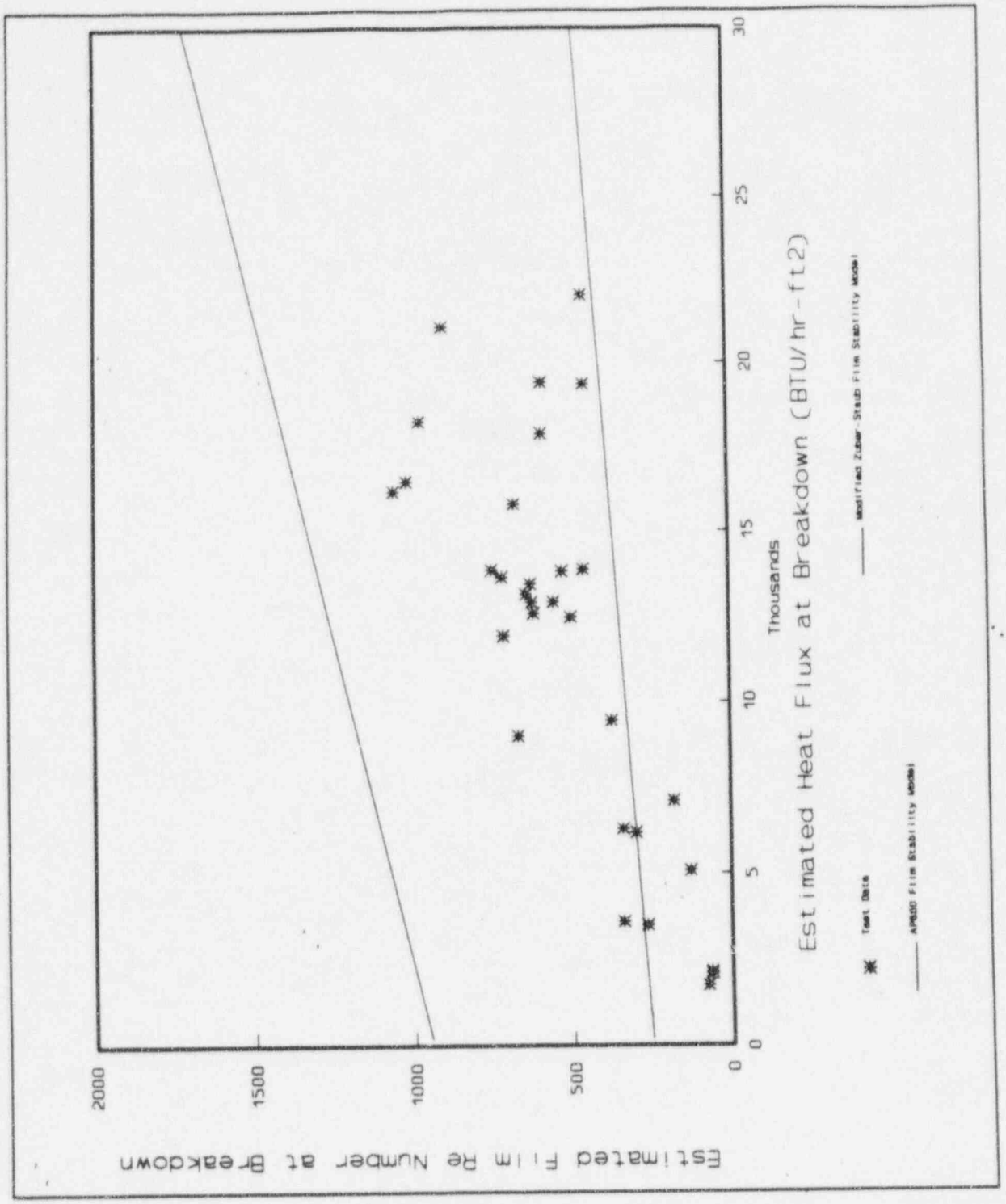

Figure 8-8 - Comparison of the Modified Zuber-Staub and AP600 Film Stability Models with LST Subcooled Film Breakdown Data

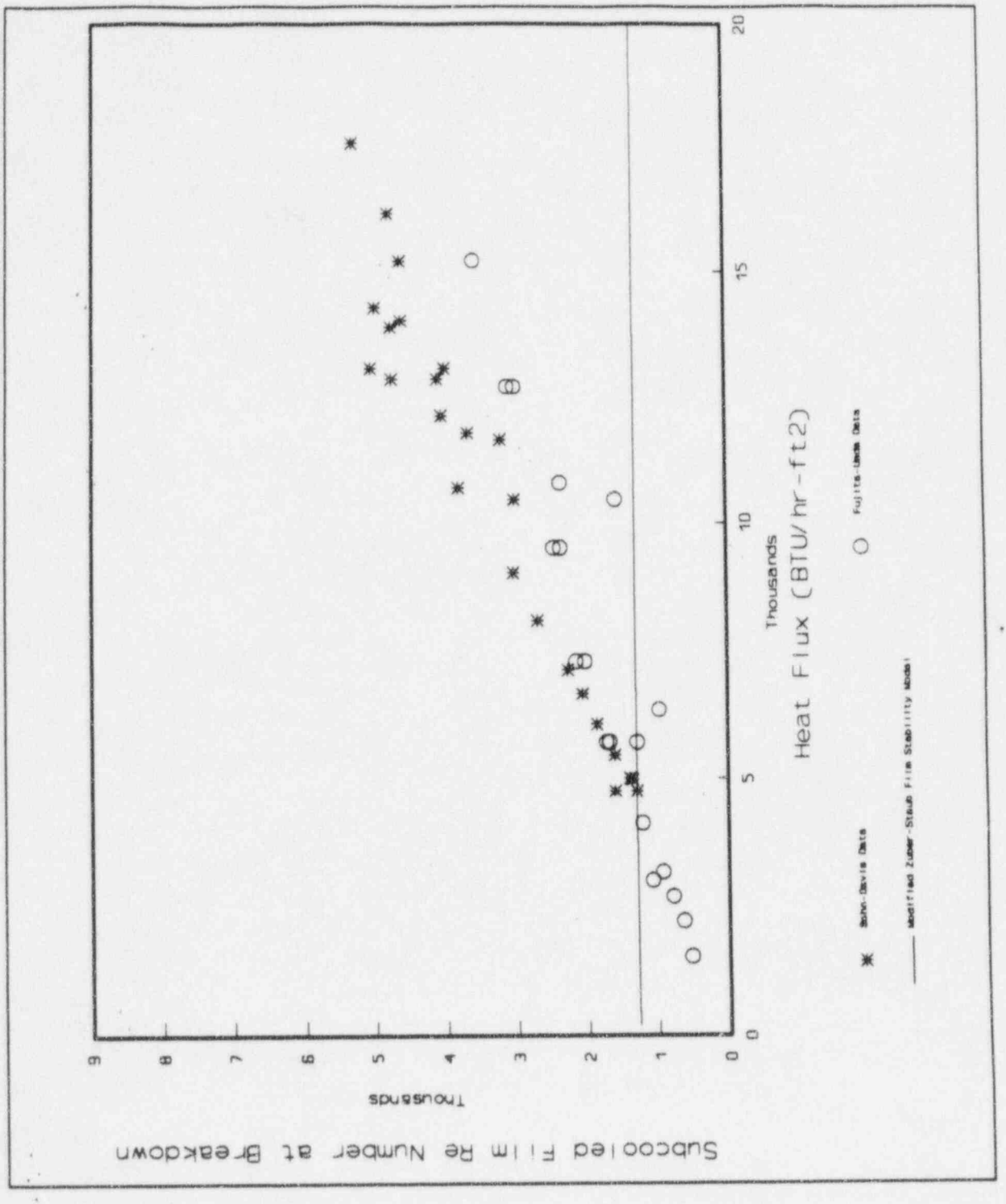

Figure 8-9 - Comparison of the Modified Zuber-Staub Film Stability Model with Other Subcooled Film Breakdown Data

The value for a bounding subcooled film stability multiplier, R_{ref}, was obtained using the film coverage test data from the unheated, full-scale Water Distribution Tests and the heated 1/8-scale Large Scale Tests. Because prototypical test data was used, R_{ref} includes the effects of subcooling, plate misalignment and the method of film application on the initial film splitting behavior. The following method was used to determine the bounding R_{ref} value.

1. The modified Zuber-Staub film stability model was used with: a contact angle of [ ]^{a,c}, the measured peak dome heat flux, the initial flow rate at the point of application, and the initial water temperature to determine a maximum value for Γ_{min}.

2. The Γ_{min} value was multiplied by R_{ref} to determine the dome circumference, CI, at which the average film flow rate became unstable.

3. The wetted coverage (width of the film stripes) at the circumference of the vessel springline, CSL, was predicted using the following approximation:

   $$WDL = (CI + CSL)/2$$

4. The predicted film coverage at the springline was compared with the measured film coverage and the R_{ref} value was varied until all of the data was bounded. Note, the film coverage was measured at the vessel gutter, not at the springline in the Large Scale Tests. Since the widths of the film stripes were observed to remain relatively constant from the springline down to the point of measurement (at the vessel gutter), the same coverage was assumed at the springline.

Using a higher film contact angle or lower film temperature in step 1 above would cause the Γ_{min} value to increase, however, this would force the bounding R_{ref} value to be lower (since the test data is bounded by the product of Γ_{min} and R_{ref}). Therefore, this method for determining the bounding coverage at the vessel springline is conservative at any contact angle.

This approach yields a bounding R_{ref} value of [ ]^{a,c}. The results are shown in Figure 8-10. The ratio of the predicted-to-measured film coverage is shown as a function of the maximum heat flux in Figure 8-11. This shows that this method for determining the initial sidewall coverage bounds the measured test coverage values over a larger range of heat flux than is expected on the AP600 shell during a DBA.

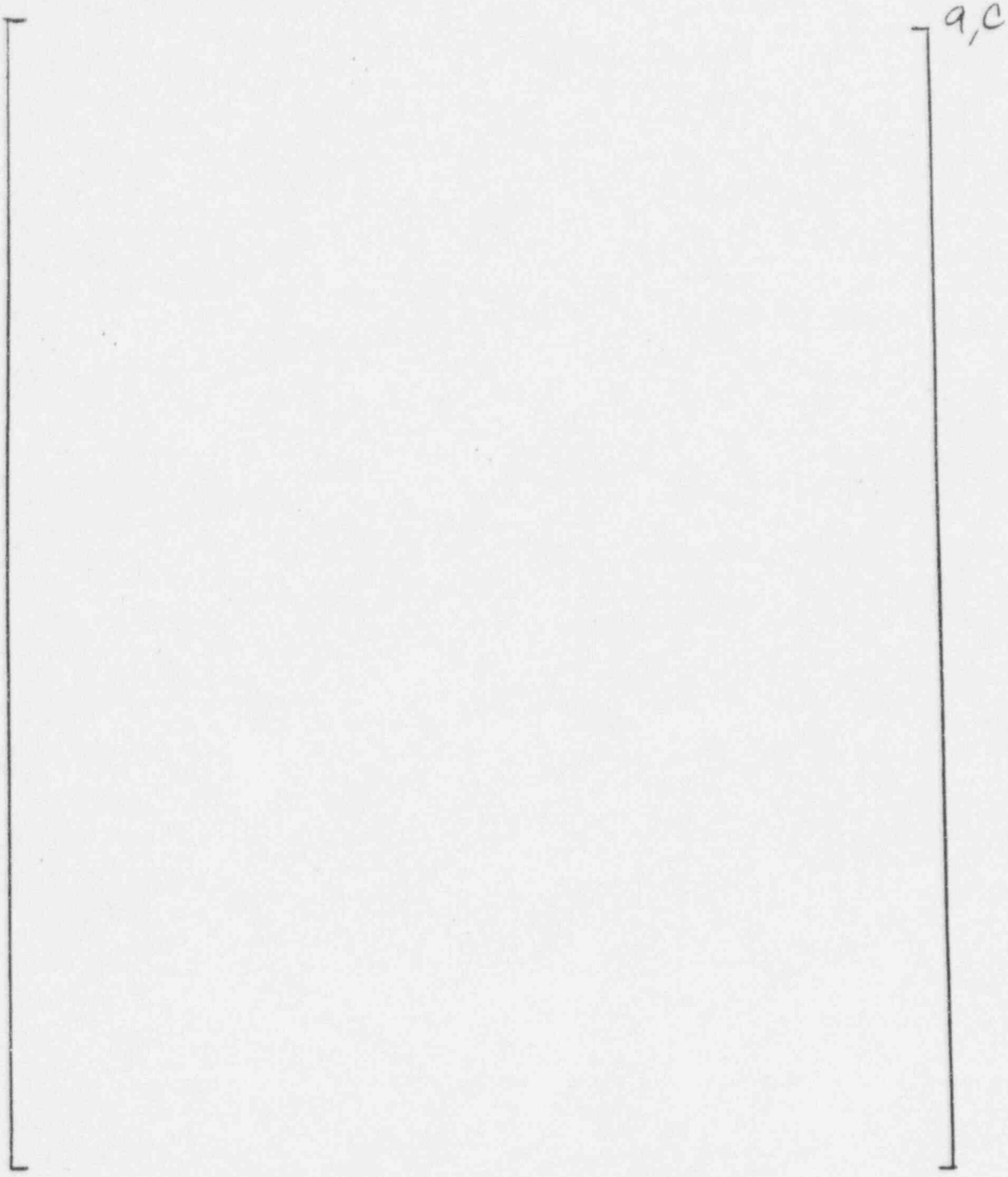

Figure 8-10 - Bounded Water Coverage Data

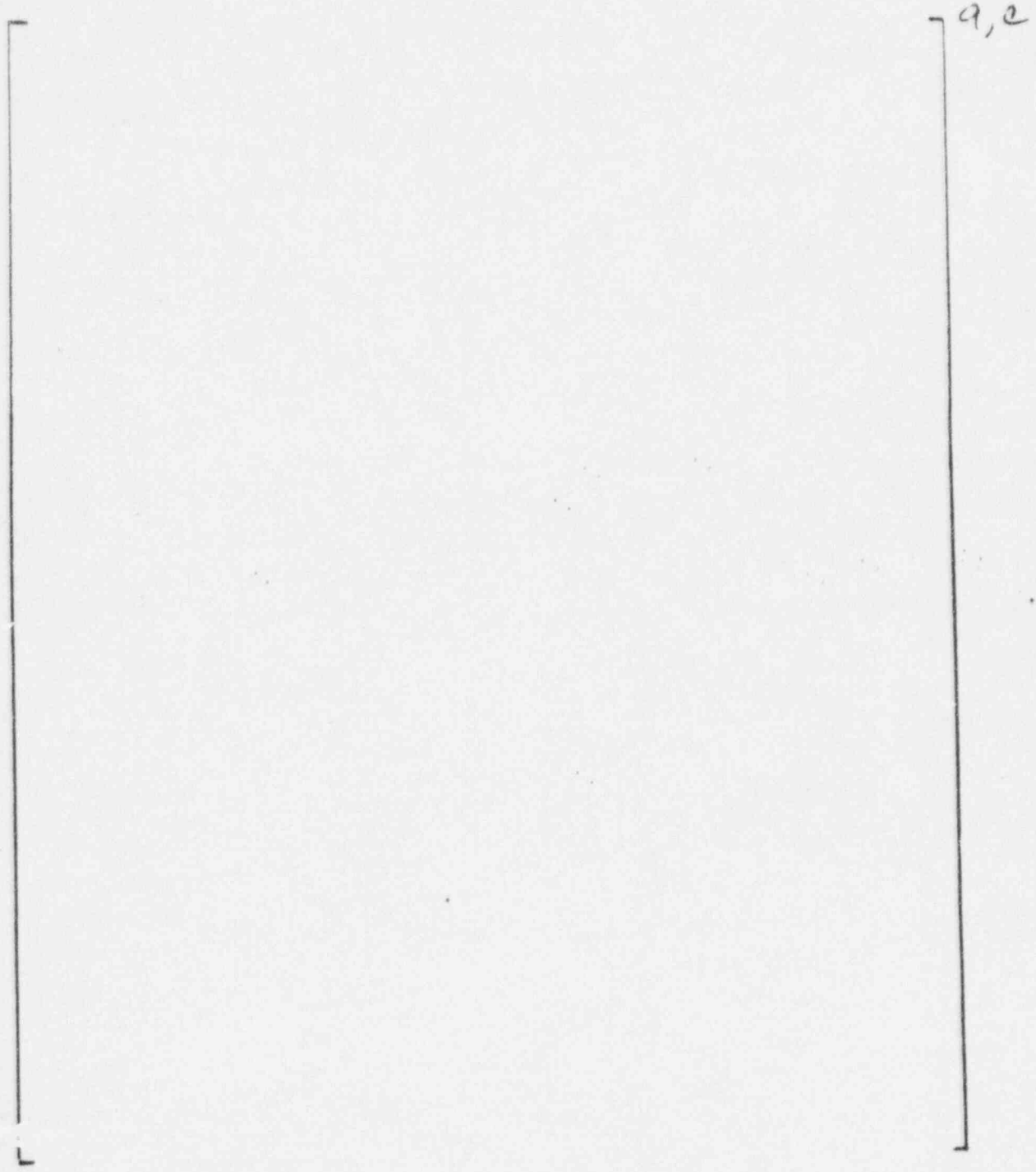

Figure 8-11 - Bounded Test Coverage Data as a Function of Heat Flux

8.5 The AP600 Containment DBA Evaluation Model Film Coverage Input

The shell evaporation rate is a function of the shell heat flux, wetted perimeter and film flow rate, all of which are interdependent and vary with time and position. The heat flux to the shell is dependent on the mass and energy release rate and the condensation rate. The shell heat flux decreases with time and increases with increasing elevation. The gravity driven water flow rate is dependent on the standpipe design and the head of water in the storage tank, and decreases with time as the storage tank drains. The film flow rate and wetted perimeter decrease with time and change with elevation as spreading and evaporation occur.

The containment DBA evaluation model requires an input water flow rate along with elevation dependent water coverage area and wetted perimeter input values to compute the evaporation rate from the shell. Because the evaluation model uses constant values for the water coverage area and wetted perimeter input at each elevation, the water flow rate input must account for changes in the evaporation rate with time.

An 11 minute delay in the application of the PCS flow is assumed. This delay is based on the maximum time required to reach steady state coverage for a PCS flow rate of 220 gpm (as determined by the Water Distribution Tests and described in Section 8.3). An estimate of the conservatism in this assumed delay time is provided in Section 8.6.3.

Water that does not evaporate on the shell will runoff. The amount of runoff will increase as the shell heat flux and coverage decrease. The AP600 film stability model is used to conservatively calculate a maximum runoff amount. This runoff amount is subtracted from the gravity driven water flow rate and the result is input to the WGOTHIC evaluation model. The method and assumptions that are used to calculate the flow rate input are described in the sample calculation that follows.

8.5.1 Sample PCS Film Flow Rate Calculation

The gravity driven PCS film flow rate is conservatively calculated assuming one of two parallel valves in the PCS piping fails to open. An example is shown in Figure 8-3.

The AP600 film stability model is used to calculate a bounding value for the minimum stable film flow rate, Γ_{mm}. The minimum stable film flow rate is shown in Figure 8-12 as a function of heat flux assuming film temperatures of 200 and 120°F (the initial film temperature) and a contact angle of [ ]^{a,c}. The value selected, [ ]^{a,c}, bounds film temperatures greater than 120°F and heat fluxes up to 10000 BTU/hr-ft^2-F.

To calculate a conservative maximum runoff flow rate, assumptions are made to minimize the wetted perimeter and maximize the film flow rate at the vessel springline. To minimize the wetted perimeter at the springline, ignore the re-distribution effect of the weirs. To maximize the film flow rate at the springline, assume the film does not evaporate on the dome.

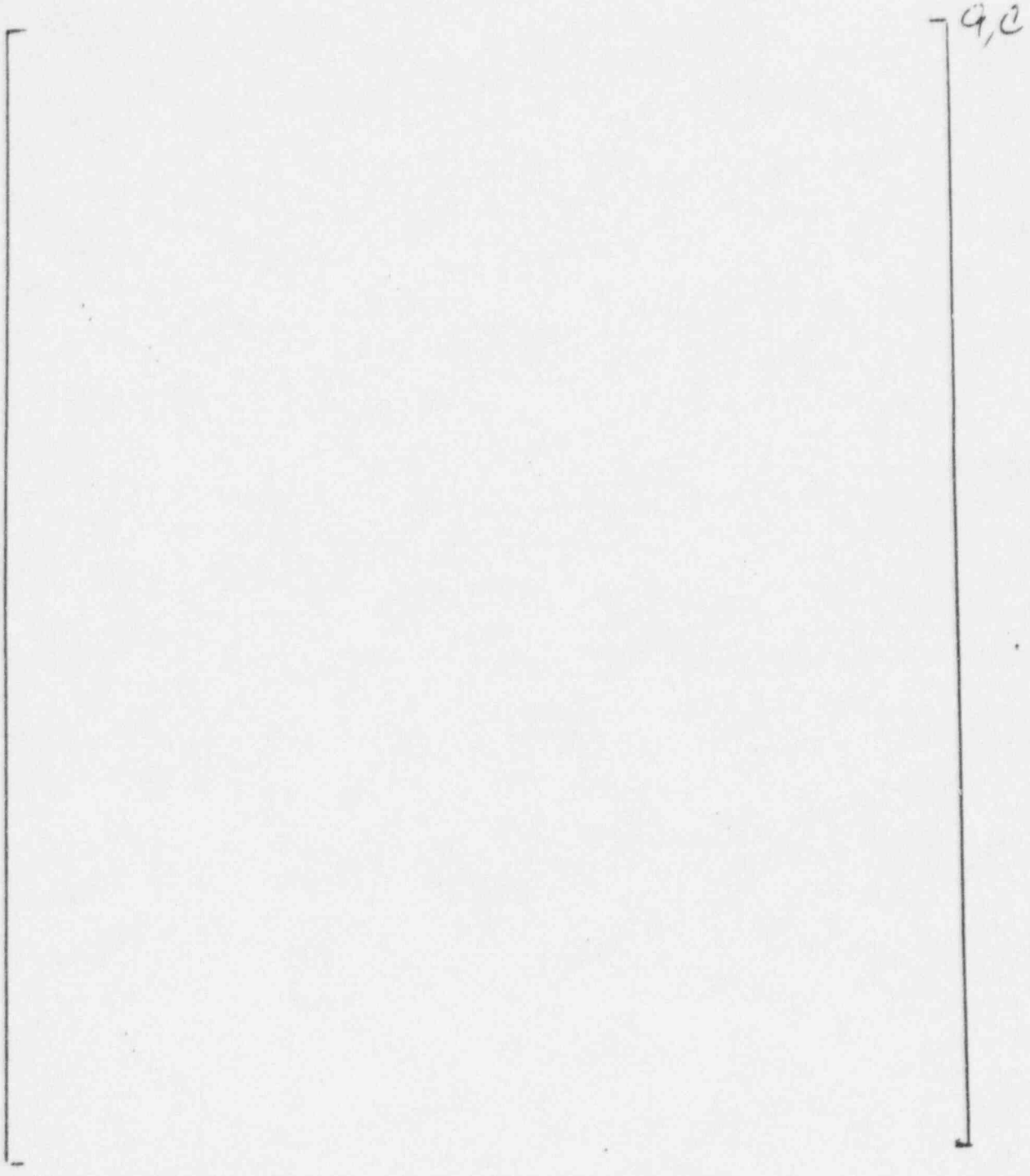

Figure 8-12 - Minimum Stable Film Flow Rates Predicted by the Zuber-Staub Model Showing Sensitivity to Heat Flux and Film Temperature at a [ ] Wetting Angle

The wetted perimeter at the springline is calculated by first determining the point on the dome where the film is predicted to become unstable

$$r_{split} = \frac{m_{PCS}}{2\pi R_{ref}\Gamma_{min}}$$

The wetted perimeter at the springline is given by the minimum of the vessel circumference, $2\pi r_{vessel}$, and

$$P_{wetted} = \pi(r_{split} + r_{vessel})$$

The film evaporates as it flows down the vertical sidewall, causing Γ to decrease. The sidewall evaporative heat flux decreases as the film travels downward. A conservatively low value for the average sidewall evaporative heat flux, Q_{avg}", is used to minimize the evaporation rate and maximize the amount of film that is calculated to run off the surface. If the average sidewall evaporative heat flux calculated by the evaluation model is less than the assumed value, the runoff amount is recalculated using the lower heat flux value and a new film flow rate is input to the evaluation model.

In the PCS tests, the film was observed to continue to thin while maintaining a relatively constant width until it was completely evaporated. For the calculation, the wetted perimeter of the evaporating film is assumed to remain constant until evaporation thins the film to a value equal to the minimum film flow rate predicted by the AP600 film stability model. The distance down the vertical sidewall at which the film reaches the stability limit, Γ_{min}, is calculated as the minimum of

$$Z_{min} = \frac{(\dot{m}_{PCS} - \Gamma_{min} P_{wetted})\, h_{fg}}{Q''_{avg} P_{wetted}}$$

and the sidewall height.

From this point on, the wetted perimeter is assumed to decrease as the film continues to evaporate at the constant stability limit, Γ_{min}. Using this assumption, the rate of change of the film flow rate with height is related to the evaporation rate

$$\Gamma_{min}\frac{dP_{wetted}}{dz} = P_{wetted}\frac{Q''_{avg}}{h_{fg}}$$

Solving for P(z) gives the exponential function

$$P(z) = P_{wetted}\, e^{-Q''_{avg} z / \Gamma_{min} h_{fg}}$$

The runoff flow rate at the bottom, Z_{max} , is

$$\dot{m}_{runoff} = \Gamma_{min} P_{wetted} e^{-Q''_{avg}(Z_{max} - Z_{min}) / \Gamma_{min} h_{fg}}$$

Alternatively, if the wetted perimeter is assumed to remain constant as the film evaporates on the vertical sidewall (more consistent with the PCS test observations), the change of the film flow rate with height would be

$$\frac{d\Gamma}{dz} = -\frac{Q''}{h_{fg}}$$

and the runoff flow rate at the bottom would be

$$\dot{m}_{runoff} = \dot{m}_{PCS} - \frac{Q'' z P_{wetted}}{h_{fg}}$$

This alternative approach results in less runoff flow, as shown in Figure 8-13. Therefore, the assumption that the film evaporates at a constant minimum stable film flow rate is more conservative.

The difference of the gravity driven PCS flow rate and the runoff flow rate is input to the AP600 containment DBA evaluation model. The calculations are summarized in Table 8-9.

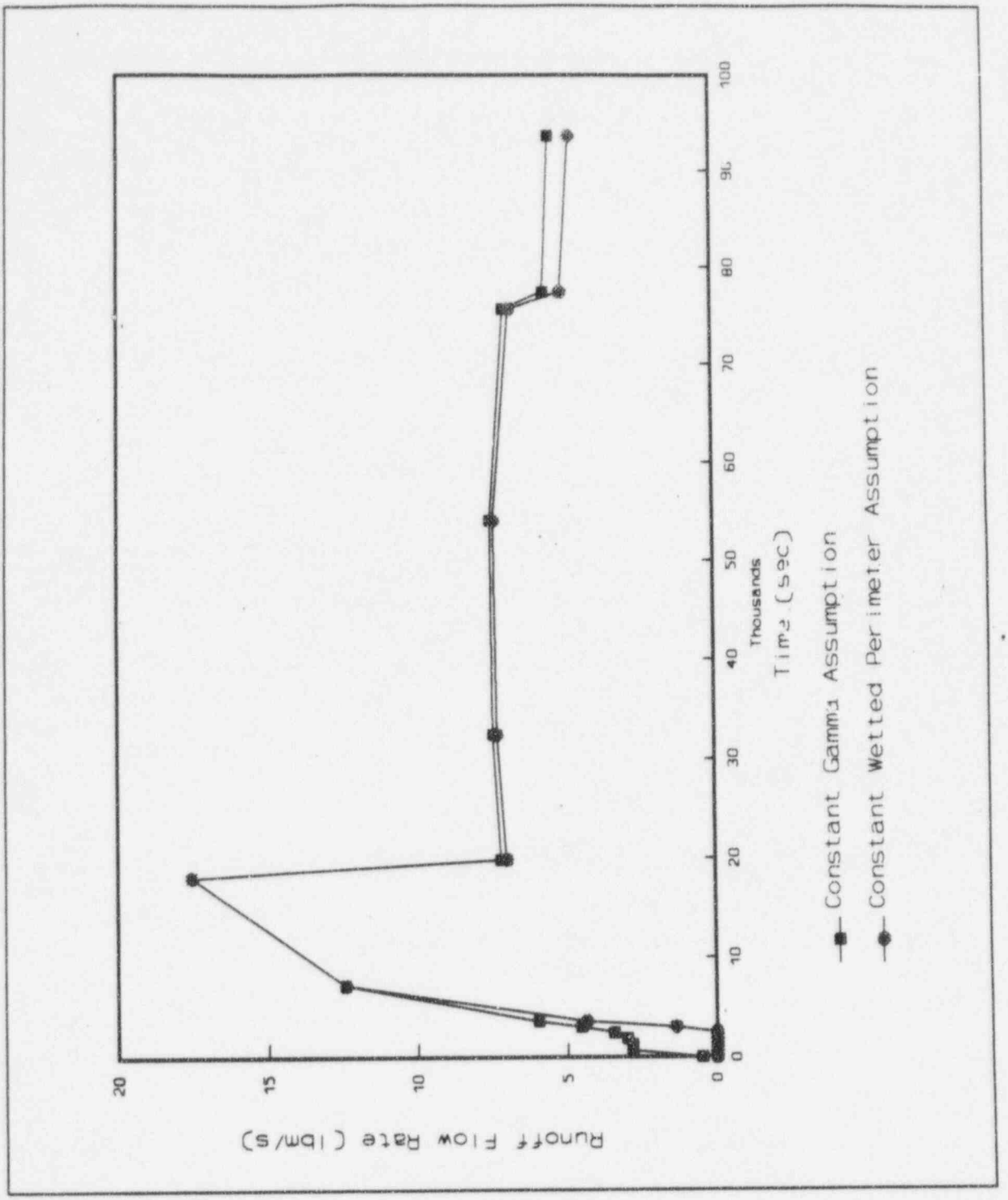

Figure 8-13 - Comparison of Predicted Runoff Flow Rates

a, c

[

]

Table 5-1 Sample Input FOS Flowrate Calculation for the DBA Evaluation Model

8.5.2 Coverage Area and Wetted Perimeter Inputs

All of the PCS film flow input to the containment DBA evaluation model should be evaporated since the predicted runoff flow rate has been maximized and subtracted from the gravity driven PCS flow rate. Therefore, the coverage area and wetted perimeter inputs to the evaluation model should be maximized to prevent runoff.

The coverage area and wetted perimeter input values for the evaluation model are based on the measured water coverage values from the unheated, phase 3 Water Distribution Tests. The coverage area percentage values listed below represent the measurements at the 27.5 gpm flow rate (which is equivalent to a 220 gpm flow rate on the AP600).

Clime	Percentage	Location
1	[ ]^{a,c}	(Top of dome to first weir)
2	[ ]^{a,c}	(Dome - between first and second weirs)
3	[ ]^{a,c}	(Dome - second weir to top of vertical sidewall)
4-7	[ ]^{a,c}	(Sidewall)

The coverage value for the top of the dome down to the first weir is estimated from the video tapes of the tests. The coverage area and wetted perimeter change significantly over the diverging area between the first and second weirs. The coverage value for this region is based on the minimum measured value just above the second weir. The coverage area and wetted perimeter do not change much over the nearly vertical region between the second weir and the top of the vertical sidewall. The coverage value for this region is based on the measured value at the springline. Based on observations from the heated large scale tests, the coverage area and wetted perimeter are assumed to remain constant down the vertical sidewall.

8.5.3 Summary of Bounding Assumptions and Conservatisms

The following list of the bounding assumptions and conservatisms in the method for determining the AP600 containment DBA evaluation model is provided for reference.

1. The gravity driven PCS flow rate is calculated assuming a single failure of one of two parallel valves in the PCS piping (Section 8.2.6). This reduces the amount of the initial water flow rate available for evaporation from the shell by about 2%.

2. A water coverage delay time is used to account for filling of the weirs and establishing steady state water coverage (Section 8.3). This neglects energy removal from the containment during the initial water coverage transient. A conservative estimate of the amount is given in Section 8.6.3.

3. The initial (applied) film temperature is assumed to be at the maximum allowable value to minimize the amount of sensible heat removal by the film.

4. The AP600 film stability model is based on a model for predicting the stability of a postulated dry spot (Section 8.4). Since film stability increases as the film temperature increases, the minimum stable film flow rate is calculated assuming the film remains at the initial (applied) temperature. Comparisons with test data for stable, evaporating films show that the stability model over-predicts the minimum measured stable film flow rates by at least a factor of 2. Comparisons with test data for subcooled films show that the stability model under-predicts the minimum stable film flow rate as the heat flux increases. A multiplier is applied to predict the breakdown of subcooled films on the dome. The value of this multiplier was determined by bounding all of the available PCS film coverage test data over a range of heat flux that is more than twice the estimated peak value during a DBA LOCA event.

5. The contact angle that is used as input to the AP600 film stability model is based on the maximum measured steady state value for a heated, weathered surface (Section 8.4.2).

6. The AP600 film stability model is used to estimate the maximum amount of runoff flow from the shell (Section 8.5.1). The redistribution effect of the weirs and the heatup and evaporation of the applied film are neglected in estimating the wetted perimeter and film flow rate at the springline. Contrary to test observations, the width of the film stripes is assumed to decrease while maintaining the predicted minimum stable film flow rate as the film evaporates on the vertical sidewall. A low estimate of the sidewall average evaporative heat flux is used to minimize the evaporation and maximize the predicted runoff flow.

7. The difference between the minimum gravity driven PCS flow rate and the maximum predicted runoff flow rate is input to the AP600 containment DBA evaluation model.

8.6 AP600 Containment DBA Evaluation Model Film Coverage Sensitivities

Sensitivitiy analyses performed with the AP600 containment DBA evaluation model are provided in this section. The models sensitivity to the location of water coverage and PCS film flow rate input are provided. An estimate of the conservatism in the assumed time delay for PCS film application is also provided.

8.6.1 Sensitivity of the Evaluation Model to the Location of Water Coverage

Calculations were performed with the WGOTHIC code to determine if the evaluation model was sensitive to the location of the water coverage. Three cases were examined. In the first case, PCS water was applied to the dome portion of the shell; in the second case, PCS water was applied to the wall portion of the shell, and in the third case, PCS water was applied to one hemisphere of the dome and wall. The input PCS water flow rate was selected to be small enough to prevent any runoff flow from the minimum surface area of the three test cases. The input PCS water flow rate was maintained at the same fixed value for each case.

Figure 8-14 compares the pressure transients for the three sensitivity cases, and clearly illustrates the insensitivity to the location of evaporation in the evaluation model. Since the input PCS flow rate is based on a conservative estimate of the evaporation rate, the coverage area input can be any value that is large enough to completely evaporate all of the flow, preventing runoff from the shell. Therefore, using coverage area input values that are based on measurements from the unheated Water Distribution Tests is reasonable.

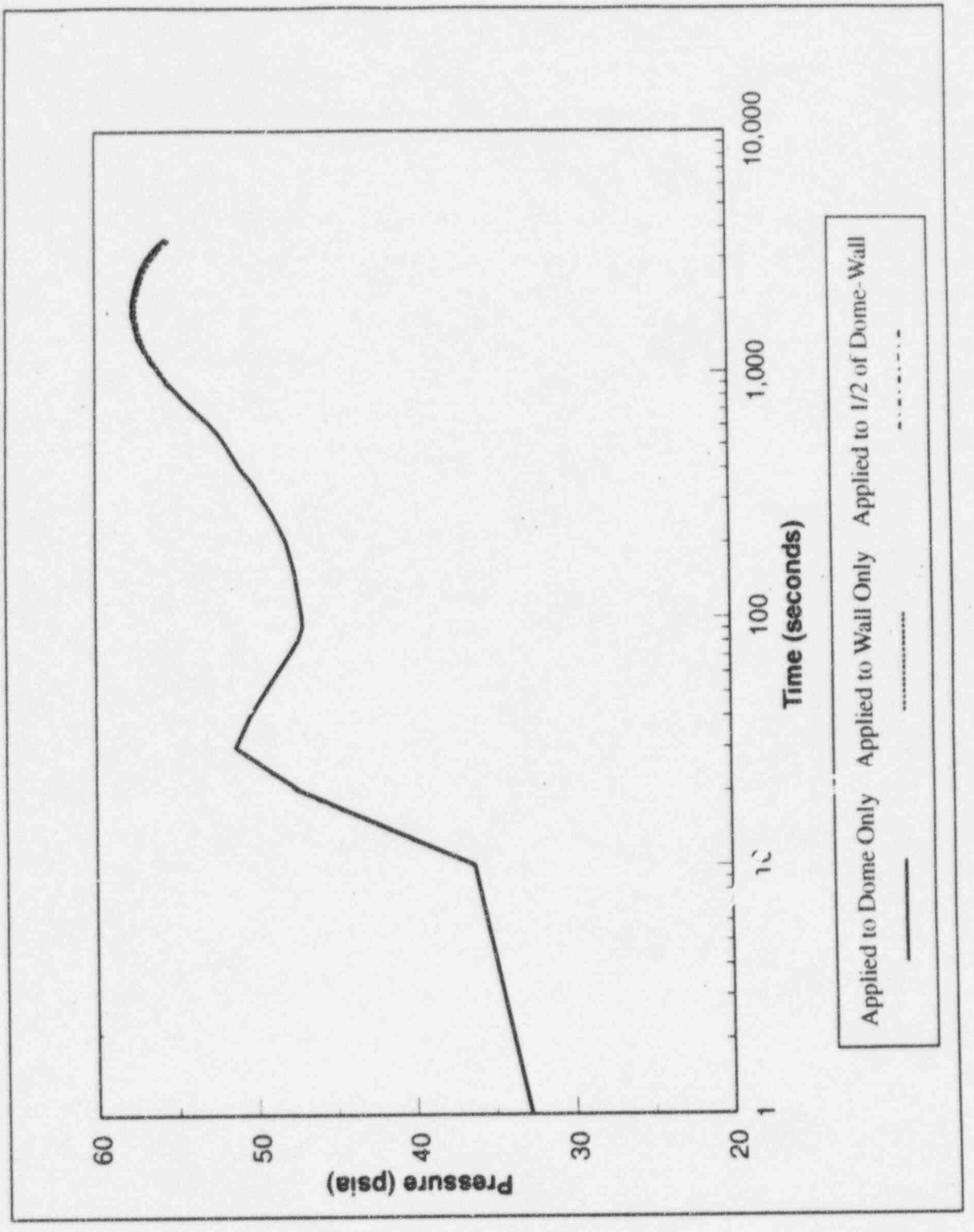

Figure 8-14 - Coverage Area Sensitivity Case Comparison of Transient Pressure

8.6.2 Sensitivity of the Evaluation Model to the Input PCS Film Flow Rate

Calculations were performed using the WGOTHIC code to determine the sensitivity of the evaluation model to the input PCS film flow rate. The nominal input PCS film flow rate was conservatively calculated, as described in Section 8.5.1. The input PCS film flow rate was increased in 10% increments from this nominal value. The time of film application was adjusted in each case to account for the increased film flow rate since the time it takes to fill the headers and weirs is inversely proportional to the film flow rate. Note, the time to reach steady state coverage after the weirs are filled (5 minutes) was conservatively assumed to be independent of the film flow rate. The coverage area and wetted perimeter input values were kept the same for each case.

Figure 8-15 presents the change in peak containment pressure as a function of the normalized change in PCS flow rate. The peak containment pressure decreases as the PCS flow rate increases from the nominal value. Increasing the PCS film flow rate does two things: it reduces the time of film application and increases the amount of evaporation from the shell. Eventually, the evaporation rate reaches a maximum value and water begins to run off the shell without evaporating. Further increases in the PCS flow rate result in diminishing reductions in the peak containment pressure.

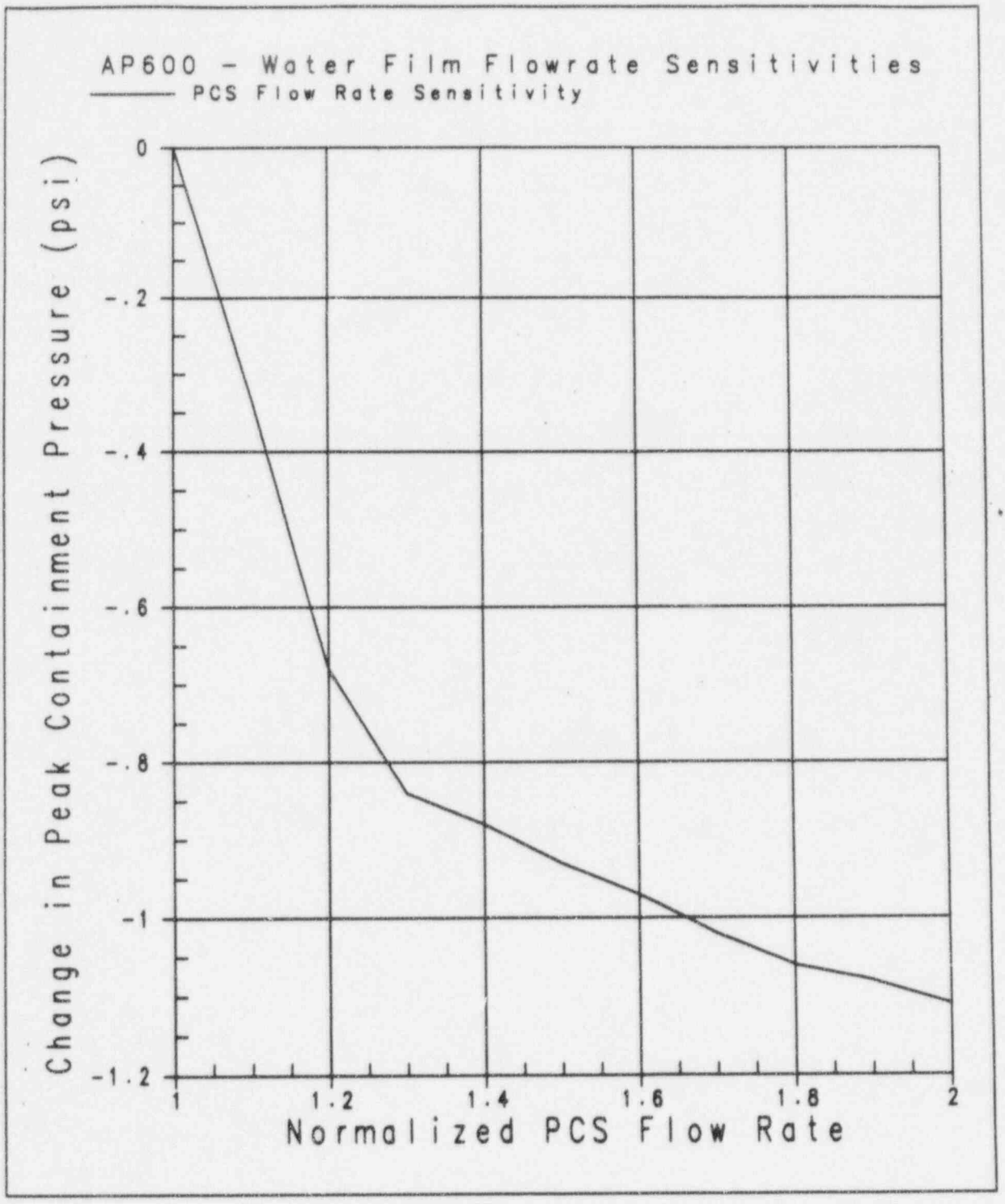

Figure 8-15 - Sensitivity to the Input PCS Film Flow Rate

8.6.3 Conservatism in the Assumed Time Delay for Application of the PCS Film

A delay in application of the PCS film is assumed in the DBA evaluation model to cover the time it takes to fill the weirs and establish a steady state coverage, as described in Section 8.3. The coverage delay time is conservative in that it neglects energy removal from the shell while steady state film coverage is being developed. An assessment of the amount of conservatism in the predicted energy removal is provided in the calculations that follow.

To quantify the amount of energy removal neglected during the development of steady state film coverage, the WGOTHIC case described in Section 8.3 was extended out to 1800 seconds. The shell temperature and heat removal results from this case were compared to the results from a second case in which the assumed water coverage delay time (for the top of the dome) was reduced to a more realistic value. For the base case, the water film was applied at 660 seconds and for the second case, the water film was applied at 60 seconds. The same input water coverage fractions were used in both cases.

Note, the WGOTHIC code assumes steady state water coverage develops instantaneously at the time the film is applied, i.e, the time required to fill the weirs and develop steady state coverage with the 220 gpm water flow rate is bounded by the assumed 660 second time delay in application of the film. Although the second case, with a more realistic estimate of the film application delay time for the top of the dome, will give a more accurate estimate of the heat removal from the top portion of the dome, it will overestimate heat removal from the rest of the dome and sidewall since the code does not model the time required to fill the weirs and establish the steady state water coverage. Therefore, only the heat removal from the top of the dome will be compared to give a minimum value for the heat removal neglected.

The transient inner and outer shell temperatures of the wet portion on the top of dome down to the first weir for both assumed PCS delay times are shown in Figure 8-16. The wet outer shell temperature increases to only about 165°F in the more accurate, 60 second delay case. It is also interesting to note that about 5 minutes after water is applied in the 660 second delay case, the wet shell temperatures decrease to about the same values as the 60 second water coverage delay case and that the difference in the coverage delay time doesn't seem to have much impact on the containment temperature.

The transient inner and outer shell temperatures for the wet and dry areas at the top of the dome for the 60 second delay case are shown in Figure 8-17. WGOTHIC models 1-D conduction (through the shell) so conduction between the wet and dry areas is neglected. If azimuthal conduction were modeled, the temperature of the dry area would be lower and the temperature of the wet area would be higher. More water would be evaporated at the higher elevations so the amount predicted to reach the lower elevations (or runoff the shell) over time would be lower. Therefore, the use of a 1-D conduction model in the evaluation model results in a higher predicted runoff flow rate and reduces the amount of evaporative heat removal from the shell.

Figures 8-18 and 8-19 compare the transient and integrated energy removal rate from the top of the dome as a function of time. There is very little difference in the energy removal rates for the first 300 seconds (due to the relatively long time constant of the shell), but the earlier application of the water film does significantly increase heat removal after 300 seconds. The heat removal rate for the 660 second delay case increases rapidly after the liquid film is applied and matches the heat removal rate of the 60 second delay case about 5 minutes later. Approximately 350,000 BTUs more energy is absorbed by the top portion of the dome due to the earlier application of water on the dome.

The energy release from the lower portions of the dome and sidewalls (if it could be calculated with the proper weir fill delay times) would cause this value to increase significantly. As an estimate, assume that all of the film applied after the first 5 minutes evaporates without running off the shell. With this assumption, an additional 10,900,000 BTUs would be absorbed from the shell. If this same amount were assumed to be removed from the containment atmosphere, it would correspond to approximately a 2 psi decrease in the peak containment pressure.

Therefore, the assumed water coverage delay time conservatively neglects the energy removal from containment during the initial water coverage transient.

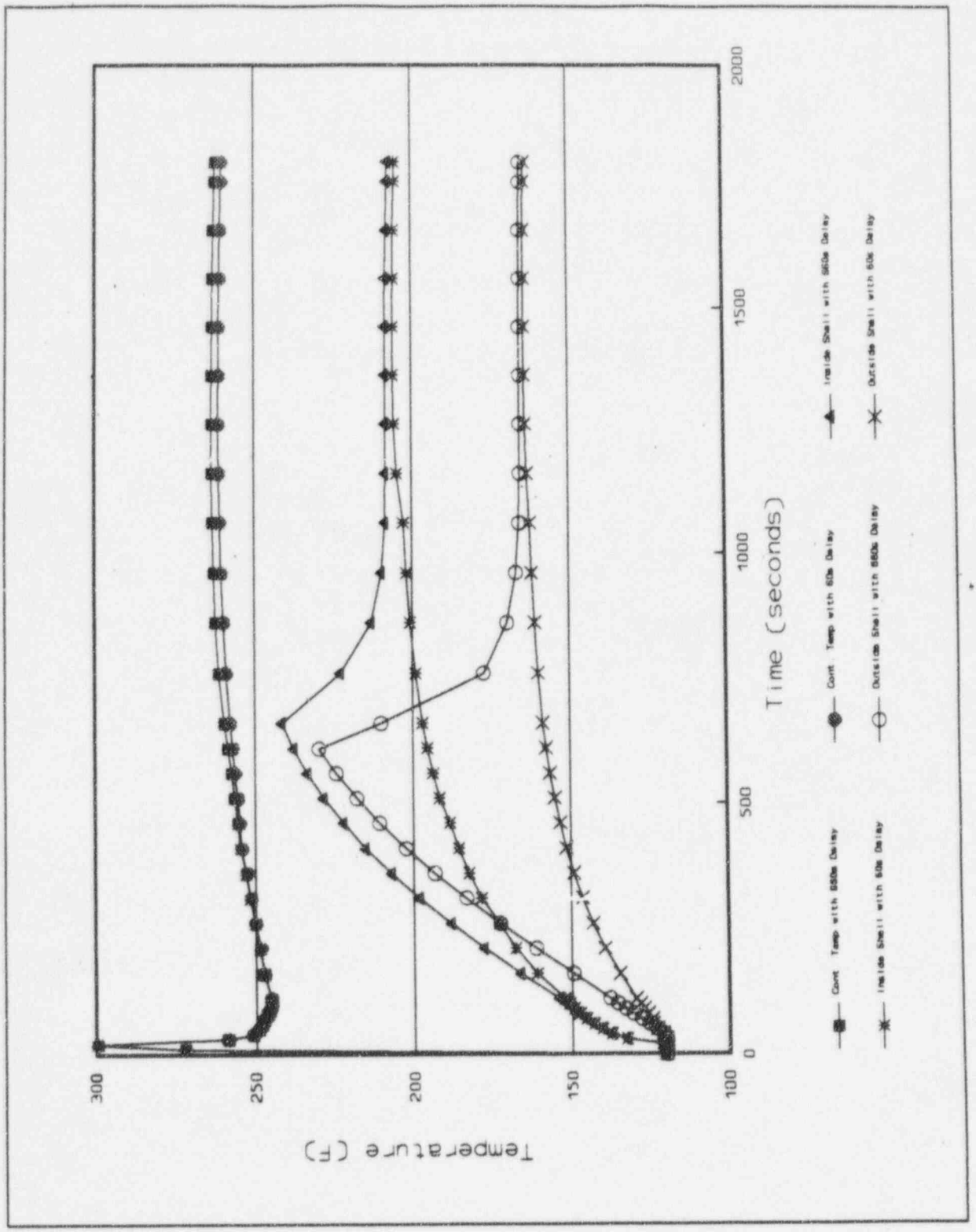

Figure 8-16 - Comparison of Wet Shell Temperatures at Top of Dome
(with PCS Film Applied at 60 and 660 Seconds)

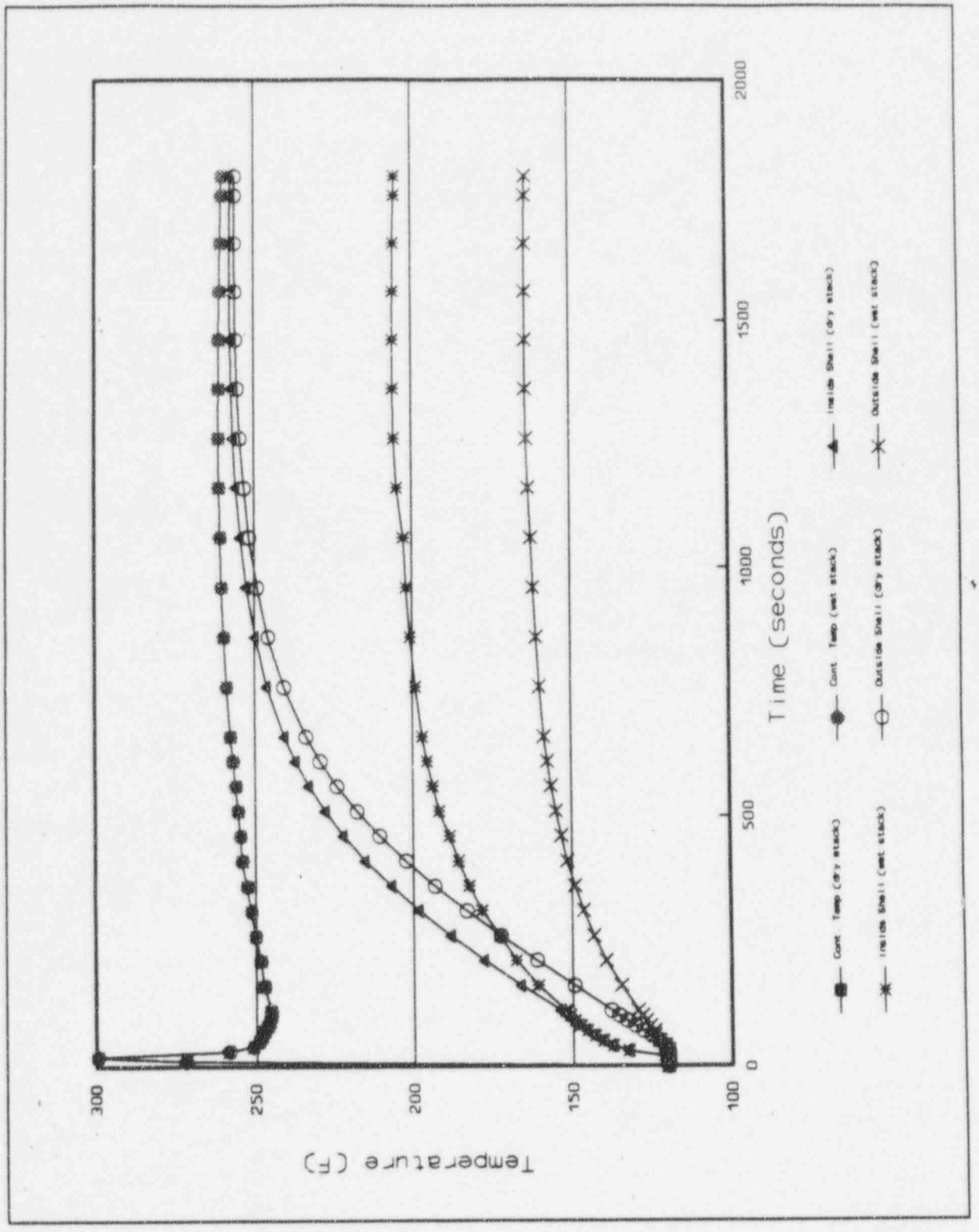

Figure 8-17 - Comparison of Wet and Dry Shell Temperatures at Top of Dome (with PCS Film Applied at 60 seconds)

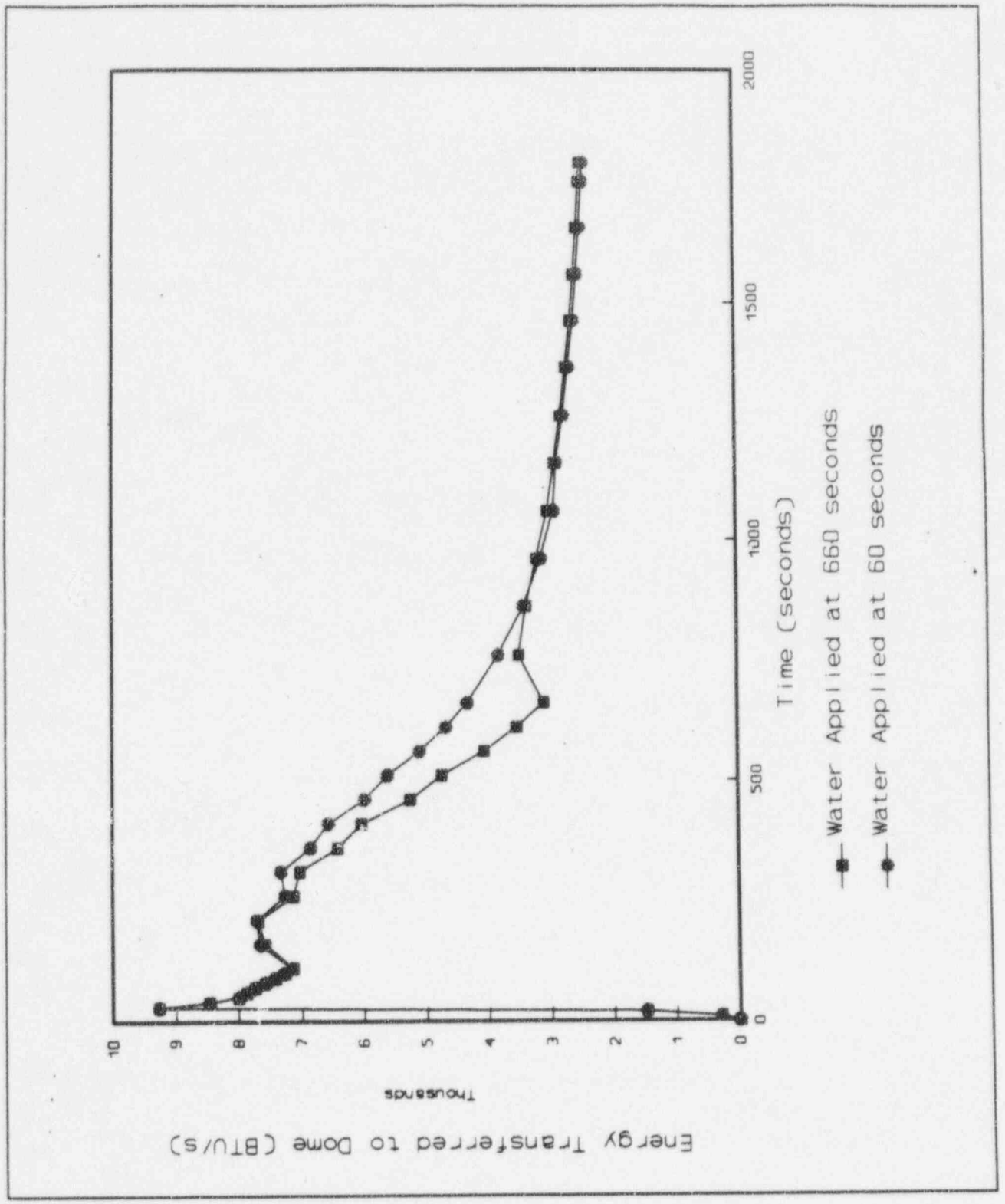

Figure 8-18 - Comparison of Energy Transferred at the Top of Dome
(with PCS Film Applied at 60 and 660 Seconds)

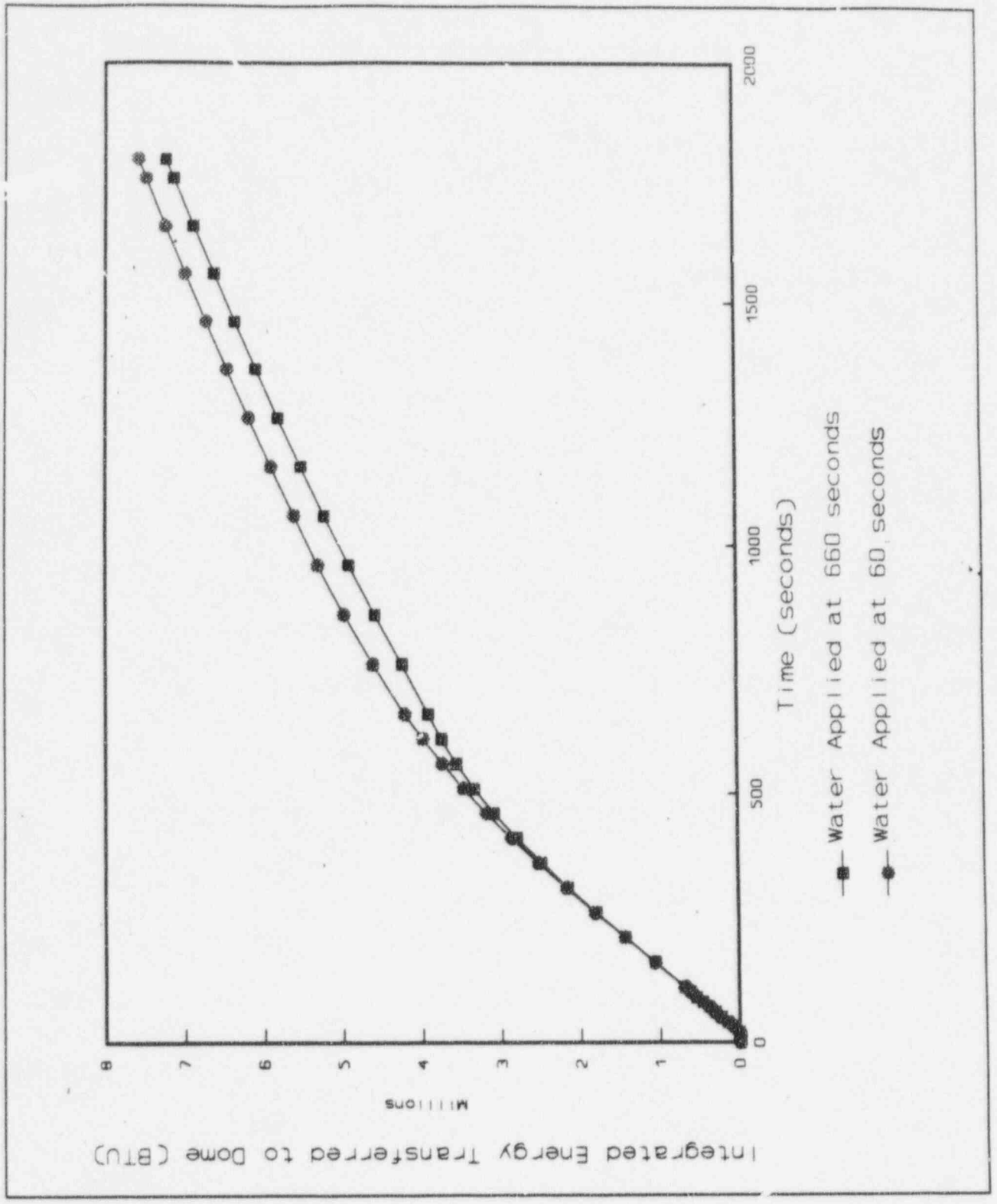

Figure 8-19 - Difference in the Integrated Energy Transferred to the Top of the Dome (with PCS Film Applied at 60 and 660 Seconds)

8.7 Summary

The range of the PCS film coverage test data parameters is tabulated and compared with the estimated range for the AP600 during a DBA. It is important for the test data to bound the maximum expected heat flux, minimum sidewall Re_{film} number and the minimum expected film temperature for evaluating the film stability model since the film is less stable at higher heat flux, lower film temperatures and lower flow rates. The test data bounds the expected range of the AP600 film parameters and is sufficient for evaluating the film stability model.

The PCS tests show that the applied water film is able to wet and rewet a hot surface (temperature exceeding 240°F) painted with the inorganic zinc coating to be used on the AP600 containment shell. Calculations of the AP600 shell temperature response, during the 10 minute time period to establish steady state water coverage, show the dry, external shell surface temperature will increase by less than 10°F at the time water first reaches the shell, by less than 50°F at the time the first weir fills and begins to spill, and by less than 70°F at the time the second weir fills and begins to spill.

A modified form of the Zuber-Staub model (for determining dry spot stability) is used to conservatively estimate a maximum value for the minimum stable film flow rate. The sensitivity of the model to contact angle, film temperature and heat flux is presented. The minimum stable film flow rate predicted by the model decreases with increasing film temperature. The minimum stable film flow rate is not sensitive to heat flux at the measured contact angle for the inorganic zinc surface.

Measurements of the film contact angle show the wettability of the inorganic zinc surface improves as it oxidizes with age. The effect of surface contamination on wettability cannot be accurately quantified, so in-service inspection and cleaning procedures will be developed to maintain surface wettability above an acceptable minimum level.

Comparisons with test data on the prototypical inorganic-zinc coated surface show the AP600 film stability model conservatively over-predicts the minimum stable film flow rates measured on the vertical test section. A multiplier, which is determined by bounding test data from the unheated Water Distribution Tests and the heated baseline and Phase 2 Large Scale Tests, is applied to the model prediction of the minimum stable film flow rate to conservatively account for subcooled film breakdown on the AP600 dome surface.

The input film flow rate is calculated to minimize the evaporation rate in the DBA evaluation model. A conservatively high film runoff flow rate is calculated using the AP600 film stability model. The difference between the gravity driven PCS flow rate and the runoff flow rate is input to the evaluation model. A sample calculation is provided to illustrate the method.

The AP600 containment DBA evaluation model is shown to be insensitive to the location of evaporation (i.e., coverage area) for a given PCS film flow rate. Therefore, the film coverage area input is based on the measured coverage fractions from the Water Distribution Tests.

References

8.1 A. T. Pieczynski, W. A. Stewart, WCAP-13884, "Water Film Formation on AP600 Reactor Containment Surface", February 1988

8.2 J. E. Gilmore, WCAP-13960, "PCS Water Distribution Phase 3 Test Data Report", December 1993

8.3 W. A. Stewart, A. T. Pieczynski, L. E. Conway, WCAP-12665 Rev 1, "Tests of Heat Transfer and Water Film Evaporation on a Heated Plate Simulating Cooling of the AP600 Reactor Containment", April 1992

8.4 R. E. Batiste, WCAP-14134, "AP600 Passive Containment Cooling System Integral Small-scale Tests Final Report", August 1994

8.6 F. E. Peters, WCAP-13566, "AP600 1/8th Large Scale Passive Containment Cooling System Heat Transfer Test Baseline Data Report", October 1992

8.7 F. E. Peters, WCAP-14135, "Final Data Report for PCS Large-Scale Tests, Phase 2 and Phase 3", July 1994

8.8 D. R. Spencer, Enclosure 2 to Westinghouse Letter NTD-NRC-94-4100, "Liquid Film Model Validation", January 1994

8.9 D. R. Spencer, WCAP-14190, "Scaling Analysis for AP600 Passive Containment Cooling System", October 1994

8.10 Frank Kreith, "Principles of Heat Transfer", 3rd Edition, 1973

8.11 W. S. Norman and V. McIntyre, "Heat Transfer to a Liquid Film on a Vertical Surface", Trans. Inst. Chem. Engrs Vol. 38, pp301-307 (1960)

8.12 V. A. Hallett, "Surface Phenomena Causing Breakdown of Falling Liquid Films During Heat Transfer", *International Journal of Heat and Mass Transfer*, Vol. 9, pp 283-294 (1966)

8.13 T. Fujita and T. Ueda, "Heat Transfer to Falling Liquid Films and Film breakdown Parts I and II", *International Journal of Heat and Mass Transfer*, Vol. 21, pp 97-108 and 109-118 (1978)

8.14 M. S. Bohn and S. H. Davis, "Thermocapillary breakdown of Falling Liquid Films at High Reynolds Numbers", *International Journal of Heat and Mass Transfer*, Vol. 36, pp 1875-1881 (1993)

8.15 S. G. Bankoff, "Dynamics and Stability of Thin Heated Liquid Films", *Transactions of the ASME - Journal of Heat Transfer*, Vol. 112, pp 538-546, (1990).

8.16 N. Zuber and F. W. Staub, "Stability of Dry Patches Forming in Liquid Films Flowing over Heated Surfaces", *International Journal of Heat and Mass Transfer*, Vol. 9, pp 897-905 (1966)

8.17 R. Wright, PCS-GSR-003, "A Method for Determining Film Flow Coverage for the AP600 Passive Containment Cooling System", July 1994

8.18 A. B. Ponter, G. A. Davies, T. K. Ross and P. G. Thornley, "The Influence of Mass Transfer on Liquid Film Breakdown", *International Journal of Heat and Mass Transfer*, Vol 10, pp 349 -359 (1966)